Do we need rebalancing strategies? A theoretical and empirical study around SMOTE and its variants.

Abdoulaye Sakho, Emmanuel Malherbe, Erwan Scornet

Do we need rebalancing strategies? A theoretical and empirical study around SMOTE and its variants.

Abdoulaye SAKHO
Artefact Research Center,
19 rue Richer Paris, France.
Sorbonne Université and Université Paris Cité,
CNRS, Laboratoire de Probabilités, Statistique
et Modélisation, F-75005 Paris, France.
abdoulaye.sakho@artefact.com

Emmanuel MALHERBE
Artefact Research Center,
19 rue Richer Paris, France.
emmanuel.malherbe@artefact.com

Erwan SCORNET
Sorbonne Université and Université Paris Cité,
CNRS, Laboratoire de Probabilités, Statistique
et Modélisation, F-75005 Paris, France.
erwan.scornet@polytechnique.edu

Abstract

Synthetic Minority Oversampling Technique (SMOTE) is a common rebalancing strategy for handling imbalanced tabular data sets. However, few works analyze SMOTE theoretically. In this paper, we prove that SMOTE (with default parameter) simply copies the original minority samples asymptotically. We also prove that SMOTE exhibits boundary artifacts, thus justifying existing SMOTE variants. Then we introduce two new SMOTE-related strategies, and compare them with state-of-the-art rebalancing procedures. Surprisingly, for most data sets, we observe that applying no rebalancing strategy is competitive in terms of predictive performances, with tuned random forests. For highly imbalanced data sets, our new method, named Multivariate Gaussian SMOTE, is competitive. Besides, our analysis sheds some lights on the behavior of common rebalancing strategies, when used in conjunction with random forests.

1 Introduction

Imbalanced data sets for binary classification are encountered in various fields such as fraud detection [Hassan and Abraham, 2016], medical diagnosis [Khalilia et al., 2011] and even churn detection [Nguyen and Duong, 2021]. In our study, we focus on imbalanced data in the context of binary classification on tabular data, for which most machine learning algorithms have a tendency to predict the majority class. This leads to biased predictions, so that several strategies have been developed in order to handle this issue, as explained by Krawczyk [2016] and Ramyachitra and Manikandan [2014]. All of these procedures can be divided into two categories: model-level and data-level approaches.

Model-level approaches modify existing classifiers in order to prevent predicting only the majority class. Among such techniques, Class-Weight (CW) works by assigning higher weights to minority samples. Another related approach is by Zhu et al. [2018] who assign data-driven weights to each tree of a random forest, in order to improve aggregated metrics such as F1 score or ROC AUC. Another model-level technique is to modify the loss function of the classifier. For instance, Cao et al. [2019] and Lin et al. [2017] introduced two new losses, respectively LDAM and Focal losses, in order to produce classifiers that better handle imbalanced data sets. However, model-level approaches are

Preprint. Under review.

not model agnostic, and thus cannot be applied to a wide variety of machine learning algorithms. Consequently, we focus in this paper on data-level approaches.

Data-level approaches can be divided into two groups: resampling strategies and synthetic procedures. Resampling techniques works by removing or copying original data points. Mani and Zhang [2003] explain that Random Under Sampling (RUS) is one of the most used resampling strategy and designed new adaptive versions called Nearmiss. RUS produces the prespecified balance between classes by dropping uniformly at random majority samples. The Nearmiss1 strategies [Mani and Zhang, 2003] includes a distinction between majority samples by ranking them using their mean distance to their nearest neighbor in the minority class. Then, low-ranked majority samples are dropped until a given balancing ratio is reached. In contrast, Random Over Sampling (ROS) duplicates original minority samples. The main default of all these sampling strategies is the fact that they either remove information from the data or do not add new information.

On the contrary, synthetic procedures generate new synthetic samples in the minority class. One of the most famous strategies in this group is *Synthetic Minority Oversampling Technique* [SMOTE, see Chawla et al., 2002][1]. In SMOTE, new minority samples are generated via linear interpolation between an original minority sample and one of its nearest neighbor in the minority class. Other approaches are based on Generative Adversarial Networks [GAN Islam and Zhang, 2020], which are computationally expensive and mostly designed for specific data structures, such as images. Random Over Sampling Examples [see Menardi and Torelli, 2014] is a variant of ROS that produces duplicated samples and then add a noise in order to get these samples slightly different from the original ones. This leads to the generation of new samples on the neighborhood of original minority samples. The main difficulty of these strategies is to synthesize relevant new samples, which must not be outliers nor simple copies of original points.

Contributions We place ourselves in the setting of imbalanced classification on tabular data, which is still very common in real-world applications Shwartz-Ziv and Armon [2022]. We prove that, without tuning the hyperparameter K (usually set to 5), SMOTE asymptotically copies the original minority samples, therefore lacking the intrinsic variability required in any synthetic generative procedure. We provide numerical illustrations of this limitation. We also establish that SMOTE density vanishes near the boundary of the support of the minority distribution, therefore justifying the introduction of SMOTE variants such as BorderLine SMOTE. Our theoretical analysis naturally leads us to introduce two SMOTE alternatives, CV-SMOTE and Multivariate Gaussian SMOTE (MGS). We evaluate and analyze both our new strategies and state-of-the-art rebalancing strategies on several real-world data sets using random forests. Through these experiments [2], we show that applying no strategy is competitive for most data sets. For the remaining data sets, our MGS procedure is promising compared to the state-of-the-art rebalancing methods, in light of its good predictive performances. Our analysis also provides some explanations about the good behavior of RUS, due to an implicit regularization in presence of random forests classifiers.

2 Related works

In this section, we focus on the literature that is the most relevant to our work: long-tail learning, SMOTE variants and theoretical studies of rebalancing strategies.

Long-tailed learning [see, e.g., Zhang et al., 2023] is a relatively new field, originally designed to handle image classification with numerous output classes. Most techniques in long-tailed learning are based on neural networks or use the large number of classes to build or adapt aggregated predictors. However, in most tabular classification data sets, the number of classes to predict is relatively small, usually equal to two [Chawla et al., 2004, He and Garcia, 2009, Grinsztajn et al., 2022]. Therefore, long-tailed learning methods are not intended for our setting as (i) we only have two output classes and (ii) state-of-the-art models for tabular data are not neural networks but tree-based methods, such as random forests or gradient boosting [see Grinsztajn et al., 2022, Shwartz-Ziv and Armon, 2022].

SMOTE has seen many variants proposed in the past decade. Several of them focus on generating synthetic samples near the boundary of the minority class support, such as ADASYN [He et al.,

[1] More than 25.000 papers found in GoogleScholar with a title including "SMOTE" over the last decade.

[2] All our experiments and our newly proposed methods can be found at `https://github.com/artefactory/smote_strategies_study`.

2008], SVM-SMOTE [Nguyen et al., 2011] or Borderline SMOTE [Han et al., 2005]. Many other variants exist such as SMOTEBoost [Chawla et al., 2003], Adaptive-SMOTE [Pan et al., 2020] or DBSMOTE [Bunkhumpornpat et al., 2012]. From a computational perspective, several synthetic methods are available in the open source package *Imb-learn* [see Lemaître et al., 2017]. Several papers study some specificities of the sampling strategies for imbalanced data sets and the impact of hyperparameter tuning. For example, Kamalov et al. [2022] study the optimal sampling ratios for imbalanced data sets when using synthetic approaches. Aguiar et al. [2023] realize a survey on imbalance data sets in the context of online learning and propose a standardized framework in order to compare rebalancing strategies in this context. Furthermore, Wongvorachan et al. [2023] aim at comparing the synthetic approaches (ROS, RUS and SMOTE) on educational data.

Several works study theoretically the rebalancing strategies. Xu et al. [2020] study the weighted risk of plug-in classifiers, for arbitrary weights. They establish rates of convergence and derive a new robust risk that may in turn improve classification performance in imbalanced scenarios. Then, based on this previous work, Aghbalou et al. [2023] derive a sharp error bound of the balanced risk for binary classification context with severe class imbalanced. Using extreme value theory, Arjovsky et al. [2022] show that applying Random Under Sampling in binary classification framework improve the worst-group error when learning from imbalanced classes with tails. Wallace and Dahabreh [2014] study the class probability estimates for several rebalancing strategies before introducing a generic methodology in order to improve all these estimates. Dal Pozzolo et al. [2015] focus on the effect of RUS on the posterior probability of the selected classifier. They show that RUS affect the accuracy and the probability calibration of the model. To the best of our knowledge, there are only few theoretical works dissecting the intrinsic machinery in SMOTE algorithm, with the notable exception of Elreedy and Atiya [2019] and Elreedy et al. [2023] who established the density of synthetic observations generated by SMOTE the associated expectation and covariance matrix.

3 A study of SMOTE

Notations We denote by $\mathcal{U}([a,b])$ the uniform distribution over $[a,b]$. We denote by $\mathcal{N}(\mu,\Sigma)$ the multivariate normal distribution of mean $\mu \in \mathbb{R}^d$ and covariance matrix $\Sigma \in \mathbb{R}^{d\times d}$. For any set A, we denote by $Vol(A)$, the Lebesgue measure of A. For any $z \in \mathbb{R}^d$ and $r > 0$, let $B(z,r)$ be the ball centered at z of radius r. We let $c_d = Vol(B(0,1))$ the volume of the unit ball in $\mathbb{R}^d$. For any $p, q \in \mathbb{N}$, and any $z \in [0,1]$, we denote by $\mathcal{B}(p,q;z) = \int_{t=0}^{z} t^{p-1}(1-t)^{q-1}\mathrm{d}t$ the incomplete beta function.

3.1 SMOTE algorithm

We assume to be given a training sample composed of N independent and identically distributed pairs (X_i, Y_i), where $X_i \in \mathbb{R}^d$ and $Y \in \{0,1\}$. We consider an imbalanced problem, in which the class $Y = 1$ is under-represented, compared to the class $Y = 0$, and thus called the minority class. We assume that we have n minority samples in our training set. In this paper, we place our theoretical and experimental studies in the context of SMOTE applied to data sets containing only *continuous* input variables.

Algorithm 1 SMOTE iteration.

Input: Minority class samples $X_1, \ldots, X_n$, number K of nearest-neighbors
Select uniformly at random X_c (called **central point**) among $X_1, \ldots, X_n$.
Denote by I the set composed of the K nearest-neighbors of X_c among $X_1, \ldots, X_n$ (w.r.t. L_2 norm).
Select $X_k \in I$ uniformly.
Sample $w \sim \mathcal{U}([0,1])$
$Z_{K,n} \leftarrow X_c + w(X_k - X_c)$
Return $Z_{K,n}$

In this section, we study the SMOTE procedure, which generates synthetic data through linear interpolations between two pairs of original samples of the minority class. SMOTE algorithm has a single hyperparameter, K, which stands for the number of nearest neighbors considered when interpolating. A single SMOTE iteration is detailed in Algorithm 1. In a classic machine learning pipeline, SMOTE procedure is repeated in order to obtain a prespecified ratio between the two classes, before training a classifier.

3.2 Theoretical results on SMOTE

SMOTE has been shown to exhibit good performances when combined to standard classification algorithms [see, e.g., Mohammed et al., 2020]. However, there exist only few works that aim at understanding theoretically SMOTE behavior. In this section, we assume that $X_1, \ldots, X_n$ are i.i.d samples from the minority class (that is, $Y_i = 1$ for all $i \in [n]$), with a common density f_X with bounded support, denoted by $\mathcal{X}$.

Lemma 3.1 (Convexity)**.** *Given f_X the distribution density of the minority class, with support $\mathcal{X}$, for all K, n, the associated SMOTE density $f_{Z_{K,n}}$ satisfies*

$$Supp(f_{Z_{K,n}}) \subseteq Conv(\mathcal{X}). \tag{1}$$

By construction, synthetic observations generated by SMOTE cannot fall outside the convex hull of $\mathcal{X}$. Equation (1) is not an equality, as SMOTE samples are the convex combination of only two original samples. For example, in dimension two, if $\mathcal{X}$ is concentrated near the vertices of a square, then SMOTE samples are distributed near the square edges, whereas Conv($\mathcal{X}$) is the whole square.

SMOTE distribution has been derived in Elreedy et al. [2023]. We build on this work and provide, in the following theorem, a different expression for the density of the data generated by SMOTE, denoted by $f_{Z_{K,n}}$. When no confusion is possible, we simply write f_Z instead of $f_{Z_{K,n}}$.

Theorem 3.2. *Let X_c be the central point chosen in a SMOTE iteration. Then, for all $x_c \in \mathcal{X}$, the random variable $Z_{K,n}$ generated by SMOTE has a conditional density $f_{Z_{K,n}}(.|X_c = x_c)$ which satisfies*

$$\begin{aligned} f_{Z_{K,n}}(z|X_c = x_c) = (n-K-1)\binom{n-1}{K} \int_0^1 \frac{1}{w^d} f_X\left(x_c + \frac{z-x_c}{w}\right) \\ \times \mathcal{B}\left(n-K-1, K; 1-\beta_{x_c,z,w}\right) \mathrm{d}w, \end{aligned} \tag{2}$$

where $\beta_{x_c,z,w} = \mu_X\left(B\left(x_c, ||z-x_c||/w\right)\right)$ and μ_X is the probability measure associated to f_X. Using the following substitution $w = \|z-x_c\|/r$, we have,

$$\begin{aligned} f_{Z_{K,n}}(z|X_c = x_c) = (n-K-1)\binom{n-1}{K} \int_{r=\|z-x_c\|}^{\infty} f_X\left(x_c + \frac{(z-x_c)r}{\|z-x_c\|}\right) \\ \times \frac{r^{d-2}\mathcal{B}\left(n-K-1, K; 1-\mu_X\left(B\left(x_c, r\right)\right)\right)}{\|z-x_c\|^{d-1}} \mathrm{d}r. \end{aligned} \tag{3}$$

Theorem 3.2 provides the expression of the density of SMOTE synthetic data conditional on the central point used to generate the new observation. The expressions established in Theorem 3.2 are very similar to Theorem 1 and Lemma 1 in Elreedy et al. [2023]. Although our proof shares the same structure as that of Elreedy et al. [2023], our starting point is different, as we consider random variables instead of geometrical arguments. The proof can be found in Section B.2.

SMOTE algorithm has only one hyperparameter K, which is the number of nearest neighbors taken into account for building the linear interpolation. By default, this parameter is set to 5. The following theorem describes the behavior of SMOTE distribution asymptotically, as $K/n \to 0$.

Theorem 3.3. *For all Borel sets $B \subset \mathbb{R}^d$, if $K/n \to 0$, as n tends to infinity, we have*

$$\lim_{n\to\infty} \mathbb{P}[Z_{K,n} \in B] = \mathbb{P}[X \in B]. \tag{4}$$

The proof of Theorem 3.3 can be found in B.3. Theorem 3.3 proves that the random variables $Z_{K,n}$ generated by SMOTE converge in distribution to the original random variable X, provided that K/n tends to zero. From a practical point of view, Theorem 3.3 guarantees asymptotically the ability of SMOTE to regenerate the distribution of the minority class. This highlights a good behavior of the default setting of SMOTE ($K = 5$), as it can create more data points, different from the original sample, and distributed as the original sample. Note that Theorem 3.3 is very generic, as it makes no assumptions on the distribution of X. A close inspection of Theorem 3.2 allows us to derive more precise bounds about the behavior of SMOTE, as established in Theorem 3.5.

Assumption 3.4. There exists $R > 0$ such that $\mathcal{X} \subset B(0, R)$. Besides, there exist $0 < C_1 < C_2 < \infty$ such that for all $x \in \mathbb{R}^d$, $C_1 \mathbb{1}_{x\in\mathcal{X}} \leq f_X(x) \leq C_2 \mathbb{1}_{x\in\mathcal{X}}$.

Theorem 3.5. *Grant Assumption 3.4. Let $x_c \in \mathcal{X}$ and $\alpha \in (0, 2R)$. For all $K \leq (n-1)\mu_X(B(x_c, \alpha))$, we have*

$$\mathbb{P}(\|Z_{K,n} - X_c\|_2 \geq \alpha | X_c = x_c) \leq \eta_{\alpha,R,d} \exp\left(-2(n-1)\left(\mu_X(B(x_c,\alpha)) - \frac{K}{n-1}\right)^2\right) \quad (5)$$

with $\eta_{\alpha,R,d} = C_2 c_d R^d \times \begin{cases} \ln\left(\frac{2R}{\alpha}\right) & \text{if } d = 1, \\ \frac{1}{d-1}\left(\left(\frac{2R}{\alpha}\right)^{d-1} - 1\right) & \text{if } d > 1. \end{cases}$

Consequently, if $\lim_{n\to\infty} K/n = 0$, we have, for all $x_c \in \mathcal{X}$, $Z_{K,n}|X_c = x_c \to x_c$ in probability.

The proof of Theorem 3.5 can be found in B.4. Theorem 3.5 establishes an upper bound on the distance between an observation generated by SMOTE and its central point. Asymptotically, when K/n tends to zero, the new synthetic observation concentrates around the central point. Recall that, by default, $K = 5$ in SMOTE algorithm. Therefore, Theorem 3.3 and Theorem 3.5 prove that, with the default settings, SMOTE asymptotically targets the original density of the minority class and generates new observations very close to the original ones. The following result establishes the characteristic distance between SMOTE observations and their central points.

Corollary 3.6. *Grant Assumption 3.4. For all $d \geq 2$, for all $\gamma \in (0, 1/d)$, we have*

$$\mathbb{P}\left[\|Z_{K,n} - X_c\|_2^2 > 12R(K/n)^\gamma\right] \leq \left(\frac{K}{n}\right)^{2/d - 2\gamma}. \quad (6)$$

The proof of Theorem 3.6 can be found in B.5 and is an adaptation of Theorem 2.4 in Biau and Devroye [2015]. The characteristic distance between a SMOTE observation and the associated central point is of order $(K/n)^{1/d}$. As expected from the curse of dimensionality, this distance increases with the dimension d. Choosing K that increases with n leads to larger characteristic distances: SMOTE observations are more distant from their central points. Theorem 3.6 leads us to choose K such that K/n does not tend to fast to zero, so that SMOTE observations are not too close to the original minority samples. However, choosing such a K can be problematic, especially near the boundary of the support, as shown in the following theorem.

Theorem 3.7. *Grant Assumption 3.4 with $\mathcal{X} = B(0, R)$. Let $\varepsilon \in (0, R)$ such that $\left(\frac{\varepsilon}{R}\right)^{1/2} \leq \frac{c_d}{\sqrt{2}dC_2}$. Then, for all $1 \leq K < n$, and all $z \in B(0,R)\backslash B(0, R-\varepsilon)$, and for all $d > 1$, we have*

$$f_{Z_{K,n}}(z) \leq C_2^{3/2}\left(\frac{2^{d+2}c_d^{1/2}}{d^{1/2}}\right)\left(\frac{n-1}{K}\right)\left(\frac{\varepsilon}{R}\right)^{1/4}. \quad (7)$$

The proof of Theorem 3.7 can be found in B.6. Theorem 3.7 establishes an upper bound of SMOTE density at points distant from less than ε from the boundary of the minority class support. More precisely, Theorem 3.7 shows that SMOTE density vanishes as $\varepsilon^{1/4}$ near the boundary of the support. Choosing $\varepsilon/R = o((K/n)^4)$ leads to a vanishing upper bound, which proves that SMOTE density is unable to reproduce the original density $f_X \geq C_1$ in the peripheral area $B(0,R)\backslash B(0, R-\varepsilon)$. Such a behavior was expected since the boundary bias of local averaging methods (kernels, nearest neighbors, decision trees) has been extensively studied [see, e.g. Jones, 1993, Arya et al., 1995, Arlot and Genuer, 2014, Mourtada et al., 2020].

For default settings of SMOTE (i.e., $K = 5$), and large sample size, this area is relatively small ($\varepsilon = o(n^{-4})$). Still, Theorem 3.7 provides a theoretical ground for understanding the behavior of SMOTE near the boundary, a phenomenon that has led to introduce variants of SMOTE to circumvent this issue [see Borderline SMOTE in Han et al., 2005]. While increasing K leads to more diversity in the generated observations (as shown in Theorem 3.5), it increases the boundary bias of SMOTE. Indeed, choosing $K = n^{3/4}$ implies a boundary effect in the peripheral area $B(0,R)\backslash B(0, R-\varepsilon)$ for $\varepsilon = o(1/n)$, which may not be negligible. Finally, note that constants in the upper bounds are of reasonable size. Letting $d = 3$, $K = 5$, $X \sim \mathcal{U}(B_d(0,1))$, the upper bound turns into $0.89n\varepsilon^{1/4}$.

3.3 Numerical illustrations

Through Section 3, we highlighted the fact that SMOTE asymptotically regenerates the distribution of the minority class, by copying the minority samples. The purpose of this section is to numerically illustrate the theoretical limitations of SMOTE procedure, typically with the default value $K = 5$.

Simulated data In order to measure the similarity between any generated data set $\mathbf{Z} = \{Z_1, \ldots, Z_m\}$ and the original data set $\mathbf{X} = \{X_1, \ldots, X_n\}$, we compute $C(\mathbf{Z}, \mathbf{X}) = \frac{1}{m}\sum_{i=1}^{m} \|Z_i - X_{(1)}(Z_i)\|_2$, where $X_{(1)}(Z_i)$ is the nearest neighbor of Z_i among $X_1, \ldots, X_n$. Intuitively, this quantity measures how far the generated data set is from the original observations: if the new data are copies of the original ones, this measure equals zero. We apply the following protocol: for each value of n,

1. Generate $\mathbf{X}$ composed of n i.i.d samples distributed as $\mathcal{U}([-3, 3]^2)$ [as in Elreedy et al., 2023].
2. Generate $\mathbf{Z}$ composed of $m = 1000$ new i.i.d observations by applying SMOTE procedure on the original data set $\mathbf{X}$, with different values of K. Compute $C(\mathbf{Z}, \mathbf{X})$.
3. Generate $\tilde{\mathbf{X}}$ composed of m i.i.d new samples distributed as $\mathcal{U}([-3, 3]^2)$. Compute $C(\tilde{\mathbf{X}}, \mathbf{X})$, which is a reference value in the ideal case of new points sampled from the same distribution.

Steps 1-3 are repeated 75 times. The average of $C(\mathbf{Z}, \mathbf{X})$ (resp. $C(\tilde{\mathbf{X}}, \mathbf{X})$) over these repetitions is computed and denoted by $\bar{C}(\mathbf{Z}, \mathbf{X})$ (resp. $\bar{C}(\tilde{\mathbf{X}}, \mathbf{X})$). We consider the metric $\bar{C}(\mathbf{Z}, \mathbf{X})/\bar{C}(\tilde{\mathbf{X}}, \mathbf{X})$, depicted in Figure 1 (see also Figure 3 in Appendix for $\bar{C}(\mathbf{Z}, \mathbf{X})$).

Results.
Figure 1 shows the renormalized quantity $\bar{C}(\mathbf{Z}, \mathbf{X})/\bar{C}(\tilde{\mathbf{X}}, \mathbf{X})$ as a function of n. We notice that the asymptotic for $K = 5$ is different since it is the only one where the distance between SMOTE data points and original data points does not vary with n. Besides, this distance is smaller than the other ones, thus stressing out that the SMOTE data points are very close to the original distribution for $K = 5$. Note that, for the other asymptotics in K, the diversity of SMOTE observations increases with n, meaning $\bar{C}(\mathbf{Z}, \mathbf{X})$ gets closer from $\bar{C}(\tilde{\mathbf{X}}, \mathbf{X})$. Besides, this diversity is asymptotically more important for $K = 0.1n$ and $K = 0.01n$. This corroborates our theoretical findings (Theorem 3.3) as these asymptotics do not satisfy $K/n \to 0$. Indeed, when K is set to a fraction of n, the SMOTE distribution does not converge to the original distribution anymore, therefore generating data points that are not simple copies of the original uniform samples. By construction SMOTE data points are close to central points which may explain why the quantity of interest in Figure 1 is smaller than 1.

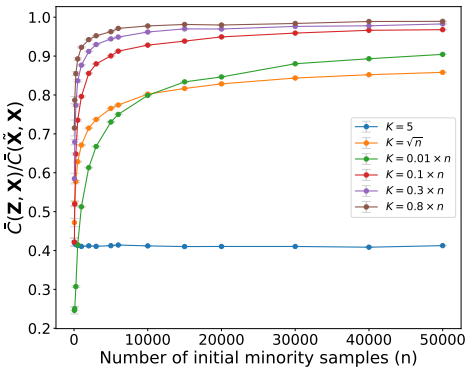

Figure 1: $\bar{C}(\mathbf{Z}, \mathbf{X})/\bar{C}(\tilde{\mathbf{X}}, \mathbf{X})$ with $\mathcal{U}([-3, 3]^2)$.

Extension to real-world data sets We extended our protocol to real-world data set. We split the data into two sets of equal size $\mathbf{X}, \tilde{\mathbf{X}}$. The first one is used for applying SMOTE strategies to sample $\mathbf{Z}$ and the other set is used to compute the normalization factor $\bar{C}(\tilde{\mathbf{X}}, \mathbf{X})$. More details about this variant of the protocol are available on Appendix A.

Results We apply the adapted protocol to Phoneme data set, described in Table 1. Figure 2 displays the quantity $\bar{C}(\mathbf{Z}, \mathbf{X})/\bar{C}(\tilde{\mathbf{X}}, \mathbf{X})$ as a function of the size n of the minority class. As in Section 3.3, we observe in Figure 2 that for the strategies, average normalized distance $\bar{C}(\mathbf{Z}, \mathbf{X})/\bar{C}(\tilde{\mathbf{X}}, \mathbf{X})$ increases except for SMOTE $K = 5$. The strategies using a value of hyperparameter K such that $K/n \to 0$ tends to converge to a value smaller than all the strategies with K such that $K/n \not\to 0$.

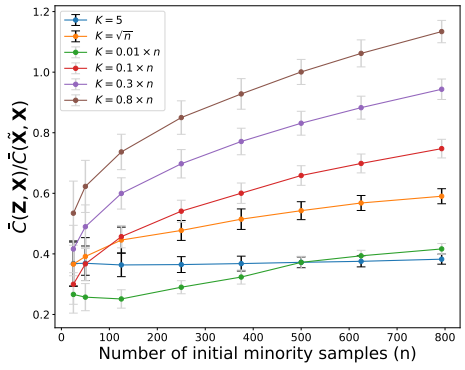

Figure 2: $\bar{C}(\mathbf{Z}, \mathbf{X})/\bar{C}(\tilde{\mathbf{X}}, \mathbf{X})$with Phoneme data.

4 Predictive evaluation on real-world data sets

In this section, we first describe the different rebalancing strategies and the two new ones we propose. Then, we describe our experimental protocol before discussing our results.

4.1 Rebalancing strategies

Class-weight (CW) The class weighting strategy assigns the same weight (choosen as hyperparameter) to each minority samples. The default setting for this strategy is to choose a weight ρ such that $\rho n = N - n$, where n and $N - n$ are respectively the number of minority and majority samples in the data set.

Over/Under Sampling strategies Random Under Sampling (RUS) acts on the majority class by selecting uniformly without replacement several samples in order to obtain a prespecified size for the majority class. Similarly, Random Over Sampling (ROS) acts on the minority class by selecting uniformly with replacement several samples to be copied in order to obtain a prespecified size for the minority class.

NearMissOne NearMissOne is an undersampling procedure. For each sample X_i in the majority class, the averaged distance of X_i to its K nearest neighbors in the minority class is computed. Then, the samples X_i are ordered according to this averaged distance. Finally, iteratively, the first X_i is dropped until the given number/ratio is reached. Consequently, the X_i with the smallest mean distance are dropped firstly.

Table 1: Initial data sets.

	N	n/N	d
Haberman	306	26%	3
Ionosphere	351	36%	32
Breast cancer	630	36%	9
Pima	768	35%	8
Vehicle	846	23%	18
Yeast	1 462	11%	8
Abalone	4 177	1%	8
Wine	4 974	4%	11
Phoneme	5 404	29%	5
MagicTel	13 376	50%	10
House_16H	22 784	30%	16
California	20 634	50%	8
CreditCard	284 315	0.2%	29

Borderline SMOTE 1 and 2 Borderline SMOTE 1 [Han et al., 2005] procedure works as follows. For each individual X_i in the minority class, let $m_-(X_i)$ be the number of samples of the majority class among the m nearest neighbors of X_i, where m is a hyperparameter. For all X_i in the minority class such that $m/2 \leq m_-(X_i) < m$, generate q successive samples $Z = WX_i + (1 - W)X_k$ where $W \sim \mathcal{U}([0, 1])$ and X_k is selected among the K nearest-neighbors of X_i in the minority class. In Borderline SMOTE 2 [Han et al., 2005], the selected neighbor X_k is chosen from the neighbors of both positive and negative classes, and Z is sampled with $W \sim \mathcal{U}([0, 0.5])$.

The limitations of SMOTE highlighted in Section 3 drive us to two new rebalancing strategies.

CV SMOTE We introduce a new algorithm, called CV SMOTE, that finds the best hyperparameter K among a prespecified grid via a 5-fold cross-validation procedure. The grid is composed of the set $\{1, 2, \ldots, 15\}$ extended with the values $\lfloor 0.01 n_{train} \rfloor$, $\lfloor 0.1 n_{train} \rfloor$, $\lfloor 0.5 n_{train} \rfloor$, $\lfloor 0.7 n_{train} \rfloor$ and $\lfloor \sqrt{n_{train}} \rfloor$, where n_{train} is the number of minority samples in the training set. Recall that through Theorem 3.5, we show that SMOTE procedure with the default value $K = 5$ asymptotically copies the original samples. The idea of CV SMOTE is then to test several (larger) values of K in order to avoid duplicating samples, therefore improving predictive performances. CV SMOTE is one of the simplest idea to solve some SMOTE limitations, which were highlighted theoretically in Section 3.

Multivariate Gaussian SMOTE(K) (MGS) We introduce a new oversampling strategy in which new samples are generated from the distribution $\mathcal{N}(\hat{\mu}, \hat{\Sigma})$, where the empirical mean $\hat{\mu}$ and covariance matrix $\hat{\Sigma}$ are estimated using the K neighbors and the central point (see Algorithm 2 for details). By default, we choose $K = d + 1$, so that estimated covariance matrices can be of full rank. MGS produces more diverse synthetic observations than SMOTE as they are spread in all directions (in case of full-rank covariance matrix) around the central point. Besides, sampling from a normal distribution may generate points outside the convex hull of the nearest neighbors.

4.2 Experiments

Initial data sets We employ classical tabular data sets already used in Grinsztajn et al. [2022]. We also used some data sets from UCI Irvine [see Dua and Graff, 2017, Grinsztajn et al., 2022] and other public data sets such as Phoneme [Alinat, 1993] and Credit Card [Dal Pozzolo et al., 2015]. All data sets are described in Table 1 and we call them *initial data sets*. As we want to compare several rebalancing methods including SMOTE, originally designed to handle continuous variables only, we have removed all categorical variables in each data set.

Algorithm 2 Multivariate Gaussian SMOTE iteration.

Input: Minority class samples $X_1, \ldots, X_n$, number K of nearest-neighbors.
Select uniformly X_c among $X_1, \ldots, X_n$.
Denote by I the set composed of the $K+1$ nearest-neighbors of X_c among $X_1, \ldots, X_n$ including X_c (w.r.t. L_2 norm).
$\hat{\mu} \leftarrow \frac{1}{K+1} \sum_{x \in I} x$
$\hat{\Sigma} \leftarrow \frac{1}{K+1} \sum_{x \in I} (x - \hat{\mu})^T (x - \hat{\mu})$
Sample $Z \sim \mathcal{N}\left(\hat{\mu}, \hat{\Sigma}\right)$
Return Z

Protocol We compare the different rebalancing strategies on the initial data sets of Table 1. We employ a 5-fold stratified cross-validation, and apply each rebalancing strategy on four training folds, in order to obtain the same number of minority/majority samples. Then, we train a Random Forest classifier [showing good predictive performance, see Grinsztajn et al., 2022]) on the same folds, and evaluate its performance on the remaining fold, via the ROC AUC. Results are averaged over the five test folds and over 100 repetitions of the cross-validation. We use the `RandomForestClassifier` module in *scikit-learn* [Pedregosa et al., 2011] and tune the tree depth via nested cross-validation Cawley and Talbot [2010]. We use the implementation of *imb-learn* [Lemaître et al., 2017] for the state-of-the-art rebalancing strategies (see Appendix A.2 for implementation details).

None is competitive for low imbalanced data sets For 10 initial data sets out of 13, applying no strategy is the best, probably highlighting that the imbalance ratio is not high enough or the learning task not difficult enough to require a tailored rebalancing strategy. Therefore, considering only continuous input variables, and measuring the predictive performance with ROC AUC, we observe that dedicated rebalancing strategies are not required for most data sets. While the performance without applying any strategy was already perceived in the literature [see, e.g., Han et al., 2005, He et al., 2008], we believe that our analysis advocates for its broad use in practice, at least as a default method. Note that for low imbalanced data sets, applying no resampling is on par with the CW strategy, one of the most common resampling strategies (regardless of tree depth tuning, see Table 4 and Table 6).

Strengthening the imbalance To analyze what could happen for data sets with higher imbalance ratio, we subsample the minority class for each one of the initial data sets mentioned above, so that the resulting imbalance ratio is set to 20%, 10% or 1% (when possible, taking into account dimension d). By doing so, we reproduce the high imbalance that is often encountered in practice [see He and Garcia, 2009]. We apply our subsampling strategy once for each data set and each imbalance ratio in a nested fashion, so that the minority samples of the 1% data set are included in the minority samples of the 10% data set. The new data sets thus obtained are called *subsampled data sets* and presented in Table 3 in Appendix A.2. For the sake of brevity, we display in Table 2 the data sets among the initial and subsampled for which the None strategy is not the best (up to its standard deviation). The others are presented in Table 4 in Appendix A.3.

Hereafter, we discuss the performances of rebalancing methods presented in Table 2. One notes that the included data sets correspond to the most imbalanced subsampling for each data set, or simply the initial data set in case of high initial imbalance. Therefore, in the following, we refer to them as *highly imbalanced data sets*.

Performances on highly imbalanced data sets Whilst in the vast majority of experiments, applying no resampling is among the best approaches to deal with imbalanced data (see Table 4), it seems to be outperformed by dedicated rebalancing strategies for highly imbalanced data sets (Table 2). Surprisingly, most rebalancing strategies do not benefit drastically from tree depth tuning, with the notable exceptions of applying no resampling and CW (see the differences between Table 2 and Table 5).

Re-weighting strategies RUS, ROS and CW are similar strategies in that they are equivalent to applying weights to the original samples. When random forests with default parameters are applied,

Table 2: Highly imbalanced data sets ROC AUC (max_depth tuned). Only data sets whose ROC AUC of at least one rebalancing strategy is larger than that of None strategy plus its standard deviation are displayed. Undersampled data sets are in italics. Standard deviations are displayed in Table 9.

Strategy	None	CW	RUS	ROS	Near Miss1	BS1	BS2	SMOTE	CV SMOTE	MGS $(d+1)$
CreditCard (0.2%)	0.966	0.967	**0.970**	0.935	0.892	0.949	0.944	0.947	0.954	0.952
Abalone (1%)	0.764	0.748	0.735	0.722	0.656	0.744	0.753	0.741	0.791	**0.802**
Phoneme (1%)	0.897	0.868	0.868	0.858	0.698	0.867	0.869	0.888	**0.924**	0.915
Yeast (1%)	0.925	0.920	0.938	0.908	0.716	0.949	0.954	**0.955**	0.942	0.945
Wine (4%)	0.928	0.925	0.915	0.924	0.682	0.933	0.927	0.934	0.938	**0.941**
Pima (20%)	0.798	**0.808**	0.799	0.790	0.777	0.793	0.788	0.789	0.787	0.787
Haberman (10%)	0.708	0.709	0.720	0.704	0.697	0.723	0.721	0.719	0.742	**0.744**
MagicTel (20%)	0.917	0.921	0.917	**0.922**	0.649	0.920	0.905	0.921	0.919	0.913
California (1%)	0.887	0.877	0.880	0.883	0.630	0.885	0.874	0.906	0.916	**0.923**

we see that ROS and CW have the same predictive performances (see Table 5). This was expected, as ROS assigns random weights to minority samples, whose expectation is that of the weights produced by CW. More importantly, RUS has better performances than both ROS and CW. This advocates for the use of RUS among these three resampling methods, as RUS produces smaller data sets, thus resulting in faster learning phases. We moreover describe another benefit of RUS in the next paragraph.

Implicit regularization The good performances of RUS, compared to ROS and CW, may result from the implicit regularization of the maximum tree depth. Indeed, fewer samples are available after the undersampling step, which makes the resulting trees shallower, as by default, each leaf contains at least one observation. When the maximum tree depth is fixed, RUS, ROS and CW strategies have the same predictive performances (see Table 7 or Table 8). Similarly, when the tree depth is tuned, the predictive performances of RUS, ROS and CW are smoothed out (see Table 2). This highlights the importance of implicit regularization on RUS good performances.

SMOTE and CV-SMOTE Default SMOTE ($K = 5$) has a tendency to duplicate original observations, as shown by Theorem 3.5. This behavior is illustrated through our experiments when the tree depth is fixed. In this context, SMOTE ($K = 5$) has the same behavior as ROS, a method that copies original samples (see Table 7 or Table 8). When the tree depth is tuned, SMOTE may exhibit better performances compared to reweighting methods (ROS, RUS, CW), probably due to a higher tree depth. Indeed, even if synthetic data are close to the original samples, they are distinct and thus allow for more splits in the tree structure. However, as expected, CV SMOTE performances are higher than default SMOTE ($K = 5$) on most data sets (see Table 2).

MGS Our second new publicly available [3] strategy exhibits good predictive performances (best performance in 4 out of 9 data sets in Table 2). This could be explained by the Gaussian sampling of synthetic observations that allows generating data points outside the convex hull of the minority class, therefore limiting the border phenomenon, established in Theorem 3.7. Note that with MGS, there is no need of tuning the tree depth: predictive performances of default RF are on par with tuned RF. Thus, MGS is a promising new strategy.

Long-tailed inspired strategies We compared in Table 14 the LDAM and Focal losses intended for long-tailed learning, using PyTorch. Table 14 shows that Focal loss performances are on par with the None strategy ones, while the performances of LDAM are significantly lower. Such methods do not seem promising for binary classification on tabular data, for which they were not initially intended.

5 Conclusion

In this paper, we analyzed the impact of rebalancing strategies on predictive performance for binary classification tasks on tabular data. First, we prove that default SMOTE simply copies the original minority samples and that it has boundary artifacts, thus justifying SMOTE variants focusing on the

[3] `https://github.com/artefactory/smote_strategies_study`

border. From a computational perspective, we show that applying no resampling is competitive for most datasets, when used in conjunction with a tuned random forest. For highly imbalanced data sets, rebalancing strategies leads to improved predictive performances, with or without tuning the maximum tree depth. Our analysis sheds some lights on the performances of reweighting strategies (ROS, RUS, CW) and an implicit regularization phenomenon occurring when such rebalancing methods are used with random forests. The SMOTE variant we propose, MGS, appears promising, with good predictive performances regardless of the hyperparameter tuning of random forests. More analyses need to be carried out in order to understand the influence of MGS parameters (regularization of the covariance matrices, number of nearest neighbors...). We also plan to extend our new MGS method to handle categorical features, and compare the different rebalancing strategies in presence of continuous and categorical input variables.

References

Anass Aghbalou, François Portier, and Anne Sabourin. Sharp error bounds for imbalanced classification: how many examples in the minority class? *arXiv preprint arXiv:2310.14826*, 2023.

Gabriel Aguiar, Bartosz Krawczyk, and Alberto Cano. A survey on learning from imbalanced data streams: taxonomy, challenges, empirical study, and reproducible experimental framework. *Machine learning*, pages 1–79, 2023.

P Alinat. Periodic progress report 4, roars project esprit ii-number 5516. *Technical Thomson Report TS ASM 93/S/EGS/NC*, 79, 1993.

Martin Arjovsky, Kamalika Chaudhuri, and David Lopez-Paz. Throwing away data improves worst-class error in imbalanced classification. *arXiv preprint arXiv:2205.11672*, 2022.

Sylvain Arlot and Robin Genuer. Analysis of purely random forests bias. *arXiv preprint arXiv:1407.3939*, 2014.

Sunil Arya, David M Mount, and Onuttom Narayan. Accounting for boundary effects in nearest neighbor searching. In *Proceedings of the eleventh annual symposium on computational geometry*, pages 336–344, 1995.

Thomas Benjamin Berrett. Modern k-nearest neighbour methods in entropy estimation, independence testing and classification. 2017. doi: 10.17863/CAM.13756. URL `https://www.repository.cam.ac.uk/handle/1810/267832`.

Gérard Biau and Luc Devroye. *Lectures on the nearest neighbor method*, volume 246. Springer, 2015.

Chumphol Bunkhumpornpat, Krung Sinapiromsaran, and Chidchanok Lursinsap. Dbsmote: density-based synthetic minority over-sampling technique. *Applied Intelligence*, 36:664–684, 2012.

Kaidi Cao, Colin Wei, Adrien Gaidon, Nikos Arechiga, and Tengyu Ma. Learning imbalanced datasets with label-distribution-aware margin loss. *Advances in neural information processing systems*, 32, 2019.

Gavin C Cawley and Nicola LC Talbot. On over-fitting in model selection and subsequent selection bias in performance evaluation. *The Journal of Machine Learning Research*, 11:2079–2107, 2010.

Nitesh V Chawla, Kevin W Bowyer, Lawrence O Hall, and W Philip Kegelmeyer. Smote: synthetic minority over-sampling technique. *Journal of artificial intelligence research*, 16:321–357, 2002.

Nitesh V Chawla, Aleksandar Lazarevic, Lawrence O Hall, and Kevin W Bowyer. Smoteboost: Improving prediction of the minority class in boosting. In *Knowledge Discovery in Databases: PKDD 2003: 7th European Conference on Principles and Practice of Knowledge Discovery in Databases, Cavtat-Dubrovnik, Croatia, September 22-26, 2003. Proceedings 7*, pages 107–119. Springer, 2003.

Nitesh V Chawla, Nathalie Japkowicz, and Aleksander Kotcz. Special issue on learning from imbalanced data sets. *ACM SIGKDD explorations newsletter*, 6(1):1–6, 2004.

Andrea Dal Pozzolo, Olivier Caelen, Reid A Johnson, and Gianluca Bontempi. Calibrating probability with undersampling for unbalanced classification. In *2015 IEEE symposium series on computational intelligence*, pages 159–166. IEEE, 2015.

Dheeru Dua and Casey Graff. Uci machine learning repository, 2017. URL `http://archive.ics.uci.edu/ml`.

Dina Elreedy and Amir F Atiya. A comprehensive analysis of synthetic minority oversampling technique (smote) for handling class imbalance. *Information Sciences*, 505:32–64, 2019.

Dina Elreedy, Amir F. Atiya, and Firuz Kamalov. A theoretical distribution analysis of synthetic minority oversampling technique (SMOTE) for imbalanced learning. *Machine Learning*, January 2023. ISSN 1573-0565. doi: 10.1007/s10994-022-06296-4. URL `https://doi.org/10.1007/s10994-022-06296-4`.

Léo Grinsztajn, Edouard Oyallon, and Gaël Varoquaux. Why do tree-based models still outperform deep learning on typical tabular data? *Advances in neural information processing systems*, 35: 507–520, 2022.

Hui Han, Wen-Yuan Wang, and Bing-Huan Mao. Borderline-smote: a new over-sampling method in imbalanced data sets learning. In *International conference on intelligent computing*, pages 878–887. Springer, 2005.

Amira Kamil Ibrahim Hassan and Ajith Abraham. Modeling insurance fraud detection using imbalanced data classification. In *Advances in Nature and Biologically Inspired Computing: Proceedings of the 7th World Congress on Nature and Biologically Inspired Computing (NaBIC2015) in Pietermaritzburg, South Africa, held December 01-03, 2015*, pages 117–127. Springer, 2016.

Haibo He and Edwardo A Garcia. Learning from imbalanced data. *IEEE Transactions on knowledge and data engineering*, 21(9):1263–1284, 2009.

Haibo He, Yang Bai, Edwardo A Garcia, and Shutao Li. Adasyn: Adaptive synthetic sampling approach for imbalanced learning. In *2008 IEEE international joint conference on neural networks (IEEE world congress on computational intelligence)*, pages 1322–1328. Ieee, 2008.

Jyoti Islam and Yanqing Zhang. Gan-based synthetic brain pet image generation. *Brain informatics*, 7:1–12, 2020.

M Chris Jones. Simple boundary correction for kernel density estimation. *Statistics and computing*, 3:135–146, 1993.

Firuz Kamalov, Amir F Atiya, and Dina Elreedy. Partial resampling of imbalanced data. *arXiv preprint arXiv:2207.04631*, 2022.

Mohammed Khalilia, Sounak Chakraborty, and Mihail Popescu. Predicting disease risks from highly imbalanced data using random forest. *BMC medical informatics and decision making*, 11:1–13, 2011.

Bartosz Krawczyk. Learning from imbalanced data: open challenges and future directions. *Progress in Artificial Intelligence*, 5(4):221–232, 2016.

Guillaume Lemaître, Fernando Nogueira, and Christos K. Aridas. Imbalanced-learn: A python toolbox to tackle the curse of imbalanced datasets in machine learning. *Journal of Machine Learning Research*, 18(17):1–5, 2017. URL `http://jmlr.org/papers/v18/16-365.html`.

Tsung-Yi Lin, Priya Goyal, Ross Girshick, Kaiming He, and Piotr Dollár. Focal loss for dense object detection. In *Proceedings of the IEEE international conference on computer vision*, pages 2980–2988, 2017.

Inderjeet Mani and I Zhang. knn approach to unbalanced data distributions: a case study involving information extraction. In *Proceedings of workshop on learning from imbalanced datasets*, volume 126, pages 1–7. ICML, 2003.

Giovanna Menardi and Nicola Torelli. Training and assessing classification rules with imbalanced data. *Data mining and knowledge discovery*, 28:92–122, 2014.

Ahmed Jameel Mohammed, Masoud Muhammed Hassan, and Dler Hussein Kadir. Improving classification performance for a novel imbalanced medical dataset using smote method. *International Journal of Advanced Trends in Computer Science and Engineering*, 9(3):3161–3172, 2020.

Jaouad Mourtada, Stéphane Gaïffas, and Erwan Scornet. Minimax optimal rates for mondrian trees and forests. *Annals of Statistics*, 48(4):2253–2276, 2020.

Hien M Nguyen, Eric W Cooper, and Katsuari Kamei. Borderline over-sampling for imbalanced data classification. *International Journal of Knowledge Engineering and Soft Data Paradigms*, 3(1): 4–21, 2011.

Nam N Nguyen and Anh T Duong. Comparison of two main approaches for handling imbalanced data in churn prediction problem. *Journal of advances in information technology*, 12(1), 2021.

Tingting Pan, Junhong Zhao, Wei Wu, and Jie Yang. Learning imbalanced datasets based on smote and gaussian distribution. *Information Sciences*, 512:1214–1233, 2020.

Fabian Pedregosa, Gaël Varoquaux, Alexandre Gramfort, Vincent Michel, Bertrand Thirion, Olivier Grisel, Mathieu Blondel, Peter Prettenhofer, Ron Weiss, Vincent Dubourg, et al. Scikit-learn: Machine learning in python. *the Journal of machine Learning research*, 12:2825–2830, 2011.

D Ramyachitra and Parasuraman Manikandan. Imbalanced dataset classification and solutions: a review. *International Journal of Computing and Business Research (IJCBR)*, 5(4):1–29, 2014.

Ravid Shwartz-Ziv and Amitai Armon. Tabular data: Deep learning is not all you need. *Information Fusion*, 81:84–90, 2022.

George Proctor Wadsworth, Joseph G Bryan, and A Cemal Eringen. Introduction to probability and random variables. *Journal of Applied Mechanics*, 28(2):319, 1961.

Byron C Wallace and Issa J Dahabreh. Improving class probability estimates for imbalanced data. *Knowledge and information systems*, 41(1):33–52, 2014.

Tarid Wongvorachan, Surina He, and Okan Bulut. A comparison of undersampling, oversampling, and smote methods for dealing with imbalanced classification in educational data mining. *Information*, 14(1):54, 2023.

Ziyu Xu, Chen Dan, Justin Khim, and Pradeep Ravikumar. Class-weighted classification: Trade-offs and robust approaches. In *International Conference on Machine Learning*, pages 10544–10554. PMLR, 2020.

Yifan Zhang, Bingyi Kang, Bryan Hooi, Shuicheng Yan, and Jiashi Feng. Deep long-tailed learning: A survey. *IEEE Transactions on Pattern Analysis and Machine Intelligence*, 2023.

Min Zhu, Jing Xia, Xiaoqing Jin, Molei Yan, Guolong Cai, Jing Yan, and Gangmin Ning. Class weights random forest algorithm for processing class imbalanced medical data. *IEEE Access*, 6: 4641–4652, 2018.

A Experiments

For all the numerical experiments, we use the following processor : AMD Ryzen Threadripper PRO 5955WX: 16 cores, 4.0 GHz, 64 MB cache, PCIe 4.0. The computer is equipped a RAM of 250Go.

A.1 Numerical illustrations

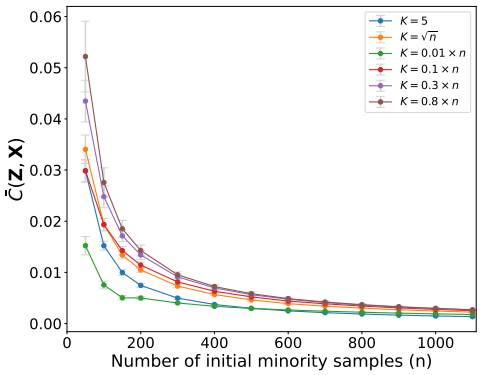

Figure 3: Average distance $\bar{C}(\mathbf{Z}, \mathbf{X})$.

Results with $\bar{C}(\mathbf{Z}, \mathbf{X})$ Figure 3 depicts the quantity $\bar{C}(\mathbf{Z}, \mathbf{X})$ as a function of the size of the minority class, for different values of K. The metric $\bar{C}(\mathbf{Z}, \mathbf{X})$ is consistently smaller for $K = 5$ than for other values of K, therefore highlighting that data generated by SMOTE with $K = 5$ are closer to the original data sample. This phenomenon is strengthened as n increases. This is an artifact of the simulation setting as the original data samples fill the input space as n increases.

More details on the numerical illustrations protocol applied to real-world data sets We apply SMOTE on real-world data and compare the distribution of the generated data points to the original distribution, using the metric $\bar{C}(\mathbf{Z}, \mathbf{X})/\bar{C}(\tilde{\mathbf{X}}, \mathbf{X})$.

For each value of n, we subsample n data points from the minority class. Then,

1. We uniformly split the data set into $X_1, \ldots, X_{n/2}$ (denoted by $\mathbf{X}$) and $\tilde{X}_1, \ldots, \tilde{X}_{n/2}$ (denoted by $\tilde{\mathbf{X}}$).
2. We generate a data set $\mathbf{Z}$ composed of $m = n/2$ i.i.d new observations $Z_1, \ldots, Z_m$ by applying SMOTE procedure on the original data set $\mathbf{X}$, with different values of K. We compute $C(\mathbf{Z}, \mathbf{X})$.
3. We use $\tilde{\mathbf{X}}$ in order to compute $C(\tilde{\mathbf{X}}, \mathbf{X})$.

This procedure is repeated $B = 100$ times to compute averages values as in Section 3.3.

A.2 Binary classification protocol

General comment on the protocol For each data set, the ratio hyperparameters of each rebalancing strategy are chosen so that the minority and majority class have the same weights in the training phase.The main purpose is to apply the strategies exactly on the same data points (X_{train}), then train the chosen classifier and evaluate the strategies on the same X_{test}. This objective is achieved by selecting each time 4 fold for the training, apply each of the strategies to these 4 exact same fold.

The state-of-the-art rebalancing strategies[see Lemaître et al., 2017] are used with their default hyperparameter values.

The subsampled data sets (see Table 3) can be obtained through the repository (the functions and the seeds are given in a jupyter notebook). For the CreditCard data set, a Time Series split is performed

Table 3: Subsampled data sets.

	N	n/N	d
Haberman (10%)	250	10%	3
Ionosphere (20%)	281	20%	32
Ionosphere (10%)	250	10%	32
Breast cancer (20%)	500	20%	9
Breast cancer (10%)	444	10%	9
Pima (20%)	625	20%	8
Vehicle (10%)	718	10%	18
Yeast (1%)	1 334	1%	8
Phoneme (20%)	4 772	20%	5
Phoneme (10%)	4 242	10%	5
Phoneme (1%)	3 856	1%	5
MagicTel (20%)	8 360	20%	10
House_16H (20%)	20 050	20%	16
House_16H (10%)	17 822	10%	16
House_16H (1%)	16 202	1%	16
California (20%)	12 896	20%	8
California (10%)	11 463	10%	8
California (1%)	10 421	1%	8

instead of a Stratified $5-$fold, because of the temporality of the data. Furthermore, a group out is applied on the different scope time value.

For MagicTel and California data sets, the initial data sets are already balanced, leading to no opportunity for applying a rebalancing strategy. This is the reason why we do not include these original data sets in our study but only their subsampled associated data sets.

The max_depth hyperparameter is tuned using GridSearch function from scikit-learn. The grids minimum is 5 and the grid maximum is the mean depth of the given strategy for the given data set (when random forest is used without tuning depth hyperparameter). Then, using numpy, a list of integer of size 8 between the minimum value and the maximum is value is built. Finally, the "None" value is added to this list.

Mean standard deviation For each protocol run, we computed the standard deviation of the ROC AUC over the 5-fold. Then, all of these 100 standard deviation are averaged in order to get what we call in some of our tables the mean standard deviations. On Table 9, Table 10 and Table 14 means standard deviation over 100 runs are displayed for each strategy (no averaging is performed).

Logistic regression Applying our study using as a classifier Logistic Regression (see Table 12), we do not observe relevant benefits of using a rebalancing strategy most of the time.

CV SMOTE We also apply our protocol for SMOTE with values of hyperparameter K depending on the number of minority inside the training set. The results are shown on both Table 11 and Table 13. As expected, CV SMOTE is most of the time the best strategy among the SMOTE variants for highly imbalanced data sets. This another illustration of our Theorem 3.5.

More results about None strategy from seminal papers Several seminal papers already noticed that the None strategy was competitive in terms of predictive performances. He et al. [2008] compare the None strategy, ADASYN and SMOTE, followed by a decision tree classifier on 5 data sets (including Vehicle, Pima, Ionosphere and Abalone). In terms of Precision and F1 score, the None strategy is on par with the two other rebalancing methods. Han et al. [2005] study the impact of Borderline SMOTE and others SMOTE variant on 4 data sets (including Pima and Haberman). The None strategy is competitive (in terms of F1 score) on two of these data sets.

The classification experiments needed 2 months of calculation time.

A.3 Additional experiments

Table 4: Remaining data sets (without those of Table 2). Random Forest (max_depth= tuned) ROC AUC for different rebalancing strategies and different data sets. Other data sets are presented in Table 2. The best strategy is highlighted in bold for each data set. Standard deviations are available on Table 10.

Strategy	None	CW	RUS	ROS	Near Miss1	BS1	BS2	SMOTE	CV SMOTE	MGS $(d+1)$
Phoneme	**0.962**	0.961	0.951	**0.962**	0.910	0.960	0.961	**0.962**	0.961	0.959
Phoneme (20%)	0.952	0.952	0.935	**0.953**	0.793	0.950	0.951	**0.953**	0.953	0.949
Phoneme (10%)	**0.936**	0.935	0.909	**0.936**	0.664	0.933	0.932	0.935	0.938	0.932
Pima	**0.833**	0.832	0.828	0.823	0.817	0.814	0.811	0.820	0.824	0.826
Yeast	0.968	**0.971**	**0.971**	0.968	0.921	0.964	0.965	0.968	0.969	0.968
Haberman	0.686	0.686	0.685	0.673	0.686	0.682	0.670	0.681	0.690	**0.698**
California (20%)	**0.956**	0.955	0.951	**0.956**	0.850	0.953	0.947	0.955	**0.956**	0.954
California (10%)	0.948	0.946	0.940	0.948	0.775	0.945	0.934	0.947	**0.950**	0.948
House_16H	**0.950**	**0.950**	0.948	**0.950**	0.899	0.945	0.942	0.948	0.949	0.948
House_16H (20%)	**0.950**	0.949	0.946	0.949	0.835	0.943	0.938	0.946	0.947	0.946
House_16H (10%)	**0.945**	0.943	0.940	0.944	0.717	0.939	0.931	0.939	0.942	0.937
House_16H (1%)	**0.906**	0.893	0.902	0.885	0.600	0.894	0.896	0.898	0.905	0.889
Vehicle	**0.995**	0.994	0.990	0.994	0.978	0.994	0.993	0.994	**0.995**	**0.995**
Vehicle (10%)	0.992	0.991	0.982	0.989	0.863	0.991	0.989	0.992	0.993	**0.994**
Ionosphere	**0.978**	**0.978**	0.974	**0.978**	0.945	**0.978**	**0.978**	**0.978**	0.977	0.976
Ionosphere (20%)	**0.988**	0.986	0.974	0.987	0.881	0.981	0.974	0.981	0.983	0.983
Ionosphere (10%)	**0.988**	0.983	0.944	0.981	0.822	0.972	0.962	0.966	0.967	0.968
Breast Cancer	**0.994**	0.993	0.993	0.993	**0.994**	0.992	0.992	0.993	**0.994**	0.993
Breast Cancer (20%)	0.996	0.995	0.994	0.995	**0.997**	0.994	0.993	0.995	0.996	0.996
Breast Cancer (10%)	**0.997**	0.996	0.994	0.996	**0.997**	0.993	0.992	0.996	**0.997**	**0.997**

Table 5: Highly imbalanced data sets. Random Forest (max_depth=∞) ROC AUC for different rebalancing strategies and different data sets. Data sets artificially undersampled for minority class are in italics. Other data sets are presented in Table 6. Mean standard deviations are computed.

Strategy	None	CW	RUS	ROS	Near Miss1	BS1	BS2	SMOTE	CV SMOTE	MGS $(d+1)$
CreditCard (0.2%) ($\pm$0.003)	0.930	0.927	**0.968**	0.932	0.887	0.933	0.941	0.950	0.961	0.953
Abalone (1%) ($\pm$0.018)	0.716	0.698	0.732	0.699	0.652	0.745	0.754	0.744	0.777	**0.805**
Phoneme (1%) ($\pm$0.020)	0.852	0.851	0.864	0.840	0.690	0.859	0.863	0.883	0.893	**0.913**
Yeast (1%) ($\pm$0.020)	0.914	0.926	0.922	0.919	0.711	0.936	**0.954**	0.936	**0.954**	0.932
Wine (4%) ($\pm$0.008)	0.926	0.923	0.917	0.927	0.693	0.934	0.927	0.934	0.935	**0.939**
Pima (20%) ($\pm$0.009)	0.777	0.791	**0.796**	0.787	0.767	0.791	0.790	0.789	0.786	0.786
Haberman (10%) ($\pm$0.028)	0.680	0.685	0.709	0.688	0.697	0.716	0.713	0.721	0.735	**0.736**
MagicTel (20%) ($\pm$0.001)	0.917	**0.921**	0.917	**0.921**	0.650	0.920	0.905	**0.921**	**0.921**	0.913
California (1%) ($\pm$0.009)	0.857	0.871	0.881	0.637	0.883	0.876	0.904	0.908	**0.921**	0.874

Table 6: Remaining data sets (without those of Table 2). Random Forest (max_depth=∞) ROC AUC for different rebalancing strategies and different data sets. Only datasets such that the None strategy is on par with the best strategies are displayed. Other data sets are presented in Table 5. Mean standard deviations are computed. The best strategy is highlighted in bold for each data set.

Strategy	None	CW	RUS	ROS	Near Miss1	BS1	BS2	SMOTE	CV SMOTE	MGS $(d+1)$
Phoneme (±0.001)	0.961	0.962	0.951	**0.963**	0.909	0.961	0.961	0.962	0.961	0.959
Phoneme (20%) (±0.002)	0.952	0.952	0.935	**0.953**	0.793	0.950	0.951	**0.953**	**0.953**	0.949
Phoneme (10%) (±0.004)	**0.937**	0.936	0.911	**0.937**	0.668	0.933	0.932	0.935	0.915	0.933
Pima (±0.005)	**0.824**	**0.824**	0.823	0.821	0.808	0.813	0.812	0.820	0.821	0.822
Yeast (±0.003)	0.965	0.969	**0.970**	0.968	0.919	0.964	0.967	0.967	0.968	0.966
Haberman (±0.017)	0.674	0.674	0.675	0.672	**0.691**	0.678	0.668	0.684	0.680	0.679
California (20%)(±0.001)	**0.956**	0.955	0.951	**0.956**	0.850	0.954	0.947	0.955	0.954	0.954
California (10%)(±0.001)	**0.948**	0.947	0.939	**0.948**	0.775	0.945	0.935	0.947	0.947	**0.948**
House_16H (±0.001)	**0.951**	0.950	0.948	0.950	0.900	0.945	0.942	0.948	0.948	0.948
House_16H (20%)(±0.001)	**0.950**	0.949	0.946	0.949	0.835	0.943	0.938	0.946	0.945	0.946
House_16H (10%)(±0.001)	**0.945**	0.943	0.941	0.944	0.718	0.939	0.931	0.939	0.939	0.937
Vehicle (±0.001)	**0.995**	0.994	0.990	**0.995**	0.977	0.994	0.994	0.994	0.994	**0.995**
Vehicle (10%) (±0.003)	0.992	0.992	0.983	0.991	0.867	0.991	0.989	0.992	0.992	**0.993**
Ionosphere (±0.003)	0.978	0.978	0.974	0.978	0.946	0.978	**0.979**	**0.979**	**0.979**	0.976
Ionosphere (20%) (±0.004)	**0.989**	0.987	0.977	0.988	0.883	0.982	0.974	0.981	0.982	0.985
Ionosphere (10%) (±0.008)	**0.989**	0.983	0.946	0.982	0.825	0.973	0.961	0.965	0.965	0.967
Breast Cancer (±0.001)	**0.994**	0.993	0.993	0.993	**0.994**	0.992	0.992	0.993	0.993	0.993
Breast Cancer (20%) (±0.001)	**0.996**	**0.996**	0.994	**0.996**	**0.996**	0.994	0.993	0.995	**0.996**	**0.996**
Breast Cancer (10%) (±0.001)	**0.997**	0.996	0.994	0.996	**0.997**	0.994	0.993	0.996	0.996	**0.997**

Table 7: Highly imbalanced data sets. ROC AUC Random Forest with max_depth=5.

Strategy	None	CW	RUS	ROS	Near Miss1	BS1	BS2	SMOTE	CV SMOTE	MGS $(d+1)$
CreditCard (0.2%)(±0.002)	0.954	0.970	0.970	0.971	0.898	0.960	0.962	**0.971**	**0.971**	0.964
Abalone (1%)(±0.017)	0.775	0.756	0.735	0.731	0.653	0.760	0.754	0.744	0.757	**0.780**
Phoneme (1%)(±0.012)	**0.891**	0.871	0.870	0.867	0.697	0.865	0.851	0.882	0.878	0.886
Yeast (1%)(±0.023)	0.923	0.921	0.934	0.887	0.709	0.933	0.922	**0.945**	0.940	0.944
Wine (4%)(±0.005)	0.900	0.905	0.900	**0.907**	0.587	0.895	0.880	0.902	0.899	0.885
Pima (20%) (±0.007)	0.802	0.811	0.805	**0.809**	0.778	0.804	0.805	0.805	0.806	0.804
Haberman (10%)(±0.029)	0.714	0.722	0.708	0.723	0.699	0.749	0.738	0.751	0.750	**0.759**
MagicTel (20%) (±0.001)	**0.893**	0.892	0.893	0.891	0.604	0.888	0.874	0.891	0.891	0.885
California (1%)(±0.008)	**0.880**	0.877	0.875	0.874	0.631	0.852	0.838	0.867	0.866	0.878

Table 8: Highly imbalanced data sets. ROC AUC Random Forest with max_depth=RUS. On the last column, the value of maximal depth when using Random forest (max_depth=∞) with RUS strategy for each data set.

Strategy	None	CW	RUS	ROS	Near Miss1	BS1	BS2	SMOTE	CV SMOTE	MGS $(d+1)$	depth
CreditCard (0.2%)(±0.002)	0.954	0.950	0.970	0.970	0.893	0.960	0.962	**0.972**	**0.972**	0.962	10
Abalone (1%) (±0.017)	0.770	0.750	0.733	0.729	0.656	0.762	0.758	0.744	0.761	**0.795**	7
Phoneme (1%)(±0.014)	**0.897**	0.874	0.872	0.869	0.695	0.869	0.858	0.887	0.880	0.894	6
Yeast (1%)(±0.021)	0.928	0.927	0.928	0.893	0.725	0.924	0.919	0.934	0.925	**0.945**	3
Wine (4%) (±0.006)	**0.927**	0.922	0.915	0.925	0.665	0.923	0.913	0.923	0.925	0.923	10
Pima (20%) (±0.009)	0.784	0.797	0.793	0.790	0.768	0.792	0.789	0.792	0.792	0.790	10
Haberman (10%) (±0.028)	0.696	0.711	0.713	0.721	0.690	0.737	0.729	0.740	0.748	**0.752**	7
MagicTel (20%) (±0.001)	0.917	0.920	0.917	0.921	0.651	0.919	0.905	**0.921**	**0.921**	0.913	20
California (1%) (±0.009)	0.895	0.871	0.877	0.875	0.639	0.876	0.859	0.884	0.903	**0.913**	10

Table 9: Table 2 with standard deviations over 100 runs. Random Forest (max_depth=tuned) ROC AUC for different rebalancing strategies and different data sets. The best strategies are displayed in bold are displayed.

Strategy	None	CW	RUS	ROS	Near Miss1	BS1	BS2	SMOTE	CV SMOTE	MGS $(d+1)$
CreditCard (0.2%)	0.966	0.967	**0.970**	0.935	0.892	0.949	0.944	0.947	0.954	0.952
std	±0.003	±0.003	±0.003	±0.003	±0.005	±0.005	±0.006	±0.004	±0.003	±0.003
Abalone (1%)	0.764	0.748	0.735	0.722	0.656	0.744	0.753	0.741	0.791	**0.802**
std	±0.021	±0.021	±0.021	±0.021	±0.033	±0.025	±0.019	±0.019	±0.018	±0.012
Phoneme (1%)	0.897	0.868	0.868	0.858	0.698	0.867	0.869	0.888	**0.924**	0.915
std	±0.015	±0.018	±0.015	±0.02	±0.030	±0.026	±0.023	±0.020	±0.014	±0.013
Yeast (1%)	0.925	0.920	0.938	0.908	0.716	0.949	0.954	**0.955**	0.942	0.945
std	±0.017	±0.030	±0.026	±0.021	±0.069	±0.0220	±0.009	±0.016	±0.021	±0.018
Wine (4%)	0.928	0.925	0.915	0.924	0.682	0.933	0.927	0.934	0.938	**0.941**
std	±0.007	±0.008	±0.005	±0.008	±0.013	±0.007	±0.008	±0.006	±0.006	±0.005
Pima (20%)	0.798	**0.808**	0.799	0.790	0.777	0.793	0.788	0.789	0.787	0.787
std	±0.009	±0.008	±0.010	±0.009	±0.007	±0.009	±0.008	±0.008	±0.007	±0.008
Haberman (10%)	0.708	0.709	0.720	0.704	0.697	0.723	0.721	0.719	0.742	**0.744**
std	±0.027	±0.029	±0.040	±0.024	±0.038	±0.027	±0.027	±0.024	±0.022	±0.026
MagicTel (20%)	0.917	0.921	0.917	**0.922**	0.649	0.920	0.905	0.921	0.919	0.913
std	±0.001	±0.001	±0.001	±0.001	±0.005	±0.001	±0.002	±0.001	±0.001	±0.001
California (1%)	0.887	0.877	0.880	0.883	0.630	0.885	0.874	0.906	0.916	**0.923**
std	±0.010	±0.013	±0.010	±0.011	±0.012	±0.014	±0.013	±0.011	±0.007	±0.006
House_16H (1%)	**0.906**	0.893	0.902	0.885	0.600	0.894	0.896	0.898	0.905	0.889
std	±0.006	±0.006	±0.006	±0.007	±0.018	±0.008	±0.006	±0.006	±0.005	±0.005

Table 10: Table 4 with standard deviations over 100 runs. Random Forest (max_depth=tuned) ROC AUC for different rebalancing strategies and different data sets. The best strategies are displayed in bold.

Strategy	None	CW	RUS	ROS	Near Miss1	BS1	BS2	SMOTE	CV SMOTE	MGS $(d+1)$
Phoneme	**0.962**	0.961	0.951	**0.962**	0.910	0.960	0.961	**0.962**	0.961	0.959
std	±0.001	±0.001	±0.001	±0.001	±0.003	±0.001	±0.001	±0.001	±0.001	±0.001
Phoneme (20%)	0.952	0.952	0.935	**0.953**	0.793	0.950	0.951	**0.953**	0.953	0.949
std	±0.001	±0.001	±0.002	±0.001	±0.014	±0.001	±0.001	±0.001	±0.001	±0.001
Phoneme (10%)	**0.936**	0.935	0.909	**0.936**	0.664	0.933	0.932	0.935	0.938	0.932
std	±0.003	±0.003	±0.005	±0.003	±0.013	±0.003	±0.004	±0.003	±0.003	±0.003
Pima	**0.833**	0.832	0.828	0.823	0.817	0.814	0.811	0.820	0.824	0.826
std	±0.004	±0.004	±0.004	±0.005	±0.004	±0.005	±0.005	±0.007	±0.006	±0.006
Yeast	0.968	**0.971**	**0.971**	0.968	0.921	0.964	0.965	0.968	0.969	0.968
std	±0.003	±0.002	±0.002	±0.004	±0.005	±0.004	±0.003	±0.004	±0.004	±0.003
Haberman	0.686	0.686	0.685	0.673	0.686	0.682	0.670	0.681	0.690	**0.698**
std	±0.020	±0.015	±0.025	±0.015	±0.012	±0.016	±0.014	±0.012	±0.015	±0.014
California (20%)	**0.956**	0.955	0.951	**0.956**	0.850	0.953	0.947	0.955	**0.956**	0.954
std	±0.001	±0.001	±0.001	±0.001	±0.002	±0.001	±0.001	±0.001	±0.001	±0.001
California (10%)	0.948	0.946	0.940	0.948	0.775	0.945	0.934	0.947	**0.950**	0.948
std	±0.002	±0.002	±0.002	±0.001	±0.004	±0.001	±0.002	±0.001	±0.001	±0.001
House_16H	**0.950**	**0.950**	0.948	**0.950**	0.899	0.945	0.942	0.948	0.949	0.948
std	±0.001	±0.001	±0.001	±0.001	±0.001	±0.001	±0.001	±0.001	±0.001	±0.001
House_16H (20%)	**0.950**	0.949	0.946	0.949	0.835	0.943	0.938	0.946	0.947	0.946
std	±0.001	±0.001	±0.001	±0.001	±0.001	±0.001	±0.001	±0.001	±0.001	±0.001
House_16H (10%)	**0.945**	0.943	0.940	0.944	0.717	0.939	0.931	0.939	0.942	0.937
std	±0.001	±0.001	±0.001	±0.001	±0.003	±0.001	±0.001	±0.001	±0.001	±0.001
House_16H	**0.906**	0.893	0.902	0.885	0.600	0.894	0.896	0.898	0.905	0.889
std	±0.006	±0.006	±0.006	±0.007	±0.018	±0.008	±0.006	±0.006	±0.005	±0.005
Vehicle	**0.995**	0.994	0.990	0.994	0.978	0.994	0.993	0.994	**0.995**	**0.995**
std	±0.001	±0.001	±0.001	±0.001	±0.003	±0.001	±0.001	±0.001	±0.001	±0.001
Vehicle (10%)	0.992	0.991	0.982	0.989	0.863	0.991	0.989	0.992	0.993	**0.994**
std	±0.002	±0.002	±0.005	±0.002	±0.010	±0.002	±0.003	±0.002	±0.001	±0.001
Ionosphere	**0.978**	**0.978**	0.974	**0.978**	0.945	**0.978**	**0.978**	**0.978**	0.977	0.976
std	±0.003	±0.003	±0.003	±0.003	±0.003	±0.003	±0.003	±0.003	±0.002	±0.002
Ionosphere (20%)	**0.988**	0.986	0.974	0.987	0.881	0.981	0.974	0.981	0.983	0.983
std	±0.002	±0.003	±0.005	±0.002	±0.013	±0.003	±0.004	±0.003	±0.004	±0.003
Ionosphere (10%)	**0.988**	0.983	0.944	0.981	0.822	0.972	0.962	0.966	0.967	0.968
std	±0.004	±0.005	±0.016	±0.005	±0.026	±0.007	±0.005	±0.005	±0.006	±0.006
Breast Cancer	**0.994**	0.993	0.993	0.993	**0.994**	0.992	0.992	0.993	**0.994**	0.993
std	±0.001	±0.001	±0.001	±0.001	±0.001	±0.001	±0.001	±0.001	±0.001	±0.001
Breast Cancer (20%)	0.996	0.995	0.994	0.995	**0.997**	0.994	0.993	0.995	0.996	0.996
std	±0.001	±0.001	±0.001	±0.001	±0.001	±0.002	±0.001	±0.001	±0.001	±0.001
Breast Cancer (10%)	**0.997**	0.996	0.994	0.996	**0.997**	0.993	0.992	0.996	**0.997**	**0.997**
std	±0.001	±0.001	±0.001	±0.001	±0.001	±0.001	±0.001	±0.001	±0.001	±0.001

Table 11: Highly imbalanced data sets at the top and remaining ones at the bottom. Random Forest (max_depth=∞) ROC AUC. The best strategy is highlighted in bold for each data set.

SMOTE Strategy	$K = 5$	$K = \sqrt{n}$	$K = 0.01n$	$K = 0.1n$	CV SMOTE
CreditCard (±0.004)	0.949	0.959	0.941	**0.961**	**0.961**
Abalone (1%)(±0.021)	0.744	0.745	0.727	0.729	**0.777**
Phoneme (1%)(±0.019)	0.883	0.880	0.872	0.871	**0.893**
Yeast (1%)(±0.016)	0.940	0.935	0.932	0.931	**0.954**
Wine (4%)(±0.006)	0.934	**0.935**	0.930	0.934	**0.935**
Pima (20%) (±0.008)	0.789	0.786	**0.790**	0.788	0.786
Haberman (10%)(±0.024)	0.721	0.723	0.715	0.725	**0.735**
MagicTel (20%)(±0.001)	**0.921**	**0.921**	**0.921**	0.920	**0.921**
California (1%)(±0.009)	0.904	0.905	0.893	0.905	**0.908**
Phoneme (±0.001)	**0.962**	0.961	**0.962**	0.961	0.961
Phoneme (20%) (±0.001)	**0.953**	0.952	**0.953**	0.952	**0.953**
Phoneme (10%) (±0.003)	0.935	0.938	0.936	**0.939**	0.915
Pima (±0.005)	0.820	0.819	**0.821**	0.819	**0.821**
Yeast (±0.003)	0.967	**0.970**	0.968	0.969	0.968
Haberman (±0.016)	**0.684**	**0.684**	0.674	0.680	0.680
California (20%)(±0.001)	**0.955**	0.954	0.954	0.953	0.954
California (10%)(±0.001)	**0.947**	**0.947**	**0.947**	0.946	**0.947**
House_16H (±0.001)	**0.948**	0.947	0.947	0.947	**0.948**
House_16H (20%)(±0.001)	**0.946**	0.944	0.945	0.944	0.945
House_16H (10%)(±0.001)	**0.939**	0.938	**0.939**	0.937	**0.939**
House_16H (1%)(±0.005)	**0.899**	0.898	0.896	0.898	0.896
Vehicle (±0.001)	**0.994**	**0.994**	**0.994**	**0.994**	**0.994**
Vehicle (10%) (±0.002)	**0.992**	**0.992**	**0.992**	**0.992**	**0.992**
Ionosphere (±0.003)	**0.979**	0.977	0.978	0.978	**0.979**
Ionosphere (20%) (±0.003)	0.981	0.981	**0.984**	0.982	0.982
Ionosphere (10%) (±0.005)	**0.965**	0.964	**0.965**	0.966	**0.965**
Breast Cancer (±0.001)	**0.993**	**0.993**	**0.993**	**0.993**	**0.993**
Breast Cancer (20%) (±0.001)	0.995	0.995	**0.996**	0.995	**0.996**
Breast Cancer (10%) (±0.001)	**0.996**	**0.996**	**0.996**	**0.996**	**0.996**

Table 12: Highly imbalanced data sets at the top and remaning ones at the bottom. Logistic Regression ROC AUC. For each data set, the best strategy is highlighted in bold and the mean of the standard deviation is computed (and rounded to 10^{-3}).

Strategy	None	CW	RUS	ROS	Near Miss1	BS1	BS2	SMOTE	CV SMOTE	MGS $(d+1)$
CreditCard (±0.001)	0.951	0.953	**0.963**	0.951	0.888	0.903	0.919	0.946	0.955	0.926
Abalone (1%) (±0.009)	0.848	0.876	0.814	0.878	0.761	0.859	0.853	0.878	**0.879**	0.872
Phoneme (1%) (±0.013)	0.800	0.804	0.792	0.804	0.695	0.783	0.779	0.805	**0.806**	0.805
Yeast (1%) (±0.006)	**0.975**	0.974	0.965	0.972	0.920	0.974	0.973	0.973	0.974	0.970
Wine (4%) (±0.003)	0.836	**0.840**	0.835	0.839	0.576	0.837	0.831	0.838	0.839	0.833
Pima (20%) (±0.005)	**0.821**	0.820	0.813	0.819	0.797	0.818	0.820	0.819	0.819	0.818
Haberman (10%) (±0.028)	0.751	**0.760**	0.726	0.758	0.750	0.750	0.746	0.753	0.754	0.743
MagicTel (20%)(±0.001)	**0.844**	0.841	0.841	0.841	0.490	0.815	0.814	0.841	0.842	0.838
California (1%) (±0.004)	0.909	0.922	0.892	0.923	0.648	0.918	0.914	**0.925**	0.924	0.923
Phoneme (±0.001)	**0.813**	0.811	0.811	0.811	0.576	0.801	0.805	0.810	0.812	0.808
Phoneme (20%) (±0.001)	**0.810**	0.808	0.807	0.808	0.505	0.801	0.805	0.807	0.809	0.805
Phoneme (10%) (±0.002)	**0.802**	0.800	0.799	0.800	0.426	0.796	0.799	0.799	0.801	0.794
Pima (±0.003)	**0.831**	**0.831**	0.828	**0.831**	0.822	0.829	0.830	0.830	0.830	0.830
Yeast (±0.001)	**0.968**	0.967	0.966	0.967	0.945	0.966	0.965	0.967	0.967	0.965
Haberman (±0.019)	0.674	0.678	0.672	0.674	**0.702**	0.663	0.661	0.674	0.670	0.674
California (20%)(±0.001)	0.927	0.927	0.926	**0.928**	0.903	**0.928**	0.925	**0.928**	**0.928**	**0.928**
California (10%)(±)	0.923	0.925	0.921	0.925	0.855	0.925	0.919	**0.926**	**0.926**	0.925
House_16H (±0.001)	0.886	**0.889**	**0.889**	**0.889**	0.867	0.888	0.888	**0.889**	**0.889**	**0.889**
House_16H (20%)(±0.001)	0.881	**0.887**	**0.887**	**0.887**	0.826	0.886	0.886	**0.887**	**0.887**	0.886
House_16H (10%)(±0.001)	0.871	**0.885**	0.884	**0.885**	0.764	**0.885**	**0.885**	**0.885**	**0.885**	0.883
House_16H (1%) (±0.006)	0.822	**0.862**	0.856	**0.862**	0.694	0.849	0.854	0.861	0.860	0.848
Vehicle (±0.001)	**0.994**	0.993	0.990	**0.994**	0.990	0.993	0.992	**0.994**	**0.994**	**0.994**
Vehicle (10%) (±0.001)	**0.994**	0.993	0.985	**0.994**	0.984	0.993	0.991	**0.994**	**0.994**	**0.994**
Ionosphere (±0.012)	0.901	0.899	**0.904**	0.893	0.872	0.889	0.889	0.894	0.895	0.897
Ionosphere (20%) (±0.021)	0.894	0.886	**0.896**	0.879	0.872	0.882	0.888	0.881	0.879	0.885
Ionosphere (10%) (±0.018)	0.862	0.856	0.857	0.858	0.812	0.868	**0.878**	0.860	0.858	0.862
Breast Cancer (±0.001)	**0.996**	**0.996**	**0.996**	**0.996**	**0.996**	**0.996**	**0.996**	**0.996**	**0.996**	**0.996**
Breast Cancer (20%) (±0.001)	**0.997**	**0.997**	**0.997**	**0.997**	**0.997**	0.996	0.994	**0.997**	**0.997**	**0.997**
Breast Cancer (10%) (±0.001)	**0.997**	**0.997**	**0.997**	**0.997**	0.996	**0.997**	**0.997**	**0.997**	**0.997**	**0.997**

Table 13: Highly imbalanced data sets at the top and remaining ones at the bottom. Logistic regression ROC AUC. For each data set, the best strategy is highlighted in bold and the mean of the standard deviation is computed (and rounded to 10^{-3}).

SMOTE Strategy	$K = 5$	$K = \sqrt{n}$	$K = 0.01n$	$K = 0.1n$	CV SMOTE
CreditCard (±0.001)	0.946	0.947	0.947	0.949	**0.955**
Abalone (1%)(±0.001)	0.878	0.878	**0.881**	0.877	0.879
Phoneme (1%)(±0.001)	0.805	0.805	**0.806**	**0.806**	**0.806**
Yeast (1%)(±0.001)	0.973	**0.974**	0.973	0.973	**0.974**
Wine (4%)(±0.003)	0.838	0.837	0.838	0.837	**0.839**
Pima (20%) (±0.005)	**0.819**	0.818	**0.819**	**0.819**	**0.819**
Haberman (10%)(±0.028)	0.753	0.749	**0.756**	0.753	0.754
MagicTel (20%)(±0.001)	0.841	0.840	0.841	0.841	**0.842**
California (1%)(±0.003)	**0.925**	**0.925**	**0.925**	**0.925**	0.924
Phoneme (±0.001)	0.810	0.810	0.810	0.810	**0.812**
Phoneme (20%) (±0.01)	0.807	0.807	0.807	0.808	**0.809**
Phoneme (10%) (±0.001)	0.799	0.799	0.799	0.799	**0.801**
Pima (±0.003)	**0.830**	**0.830**	**0.830**	**0.830**	**0.830**
Yeast (±0.001)	**0.967**	**0.967**	**0.967**	**0.967**	**0.967**
Haberman (±0.018)	0.674	0.677	**0.678**	0.677	0.670
California (20%)(±0.001)	**0.928**	**0.928**	**0.928**	**0.928**	**0.928**
California (10%)(±0.001)	**0.926**	**0.926**	**0.926**	0.925	**0.926**
House_16H(±0.001)	**0.889**	**0.889**	**0.889**	**0.889**	**0.889**
House_16H (20%)(±0.001)	**0.887**	**0.887**	**0.887**	0.886	**0.887**
House_16H (10%)(±0.001)	**0.885**	**0.885**	**0.885**	0.884	**0.885**
House_16H (1%)(±0.005)	**0.861**	0.860	0.859	0.859	0.860
Vehicle (±0.001)	**0.994**	**0.994**	**0.994**	**0.994**	**0.994**
Vehicle (10%) (±0.001)	**0.994**	**0.994**	**0.994**	**0.994**	**0.994**
Ionosphere (±0.011)	0.894	**0.896**	0.895	0.894	0.895
Ionosphere (20%) (±0.20)	**0.881**	**0.881**	0.879	0.880	0.879
Ionosphere (10%) (±0.017)	0.860	0.857	**0.861**	0.859	0.858
Breast Cancer (±0.001)	**0.996**	**0.996**	**0.996**	**0.996**	**0.996**
Breast Cancer (20%) (±0.001)	**0.997**	**0.997**	**0.997**	**0.997**	**0.997**
Breast Cancer (10%) (±0.001)	**0.997**	**0.997**	**0.997**	**0.997**	**0.997**

Table 14: Highly imbalanced data sets ROC AUC. Logistic regression reimplemented in PyTorch using the implementation of Cao et al. [2019].

Strategy	None	LDAM loss	Focal loss
CreditCard	$\mathbf{0.968} \pm 0.002$	0.934 ± 0.003	0.967 ± 0.002
Abalone (1%)	0.790 ± 0.008	0.735 ± 0.046	$\mathbf{0.799} \pm 0.009$
Phoneme (1%)	0.806 ± 0.008	0.656 ± 0.091	$\mathbf{0.807} \pm 0.008$
Yeast (1%)	$\mathbf{0.977} \pm 0.002$	0.942 ± 0.002	$\mathbf{0.977} \pm 0.002$
Wine (4%)	0.827 ± 0.002	0.675 ± 0.087	$\mathbf{0.831} \pm 0.002$
Pima (20%)	$\mathbf{0.821} \pm 0.005$	0.697 ± 0.036	$\mathbf{0.821} \pm 0.005$
Haberman (10%)	0.749 ± 0.030	0.611 ± 0.077	$\mathbf{0.750} \pm 0.029$
MagicTel(20%)	0.843 ± 0.001	0.785 ± 0.20	$\mathbf{0.844} \pm 0.001$
California(1%)	0.833 ± 0.006	$\mathbf{0.922} \pm 0.003$	0.841 ± 0.007

B Main proofs

This section contains the main proof of our theoretical results. The technicals lemmas used by several proofs are available on Appendix C.

B.1 Proof of Theorem 3.1

Proof of Theorem 3.1. Let $\mathcal{X}$ be the support of P_X. SMOTE generates new points by linear interpolation of the original minority sample. This means that for all x, y in the minority samples or generated by SMOTE procedure, we have $(1-t)x + ty \in Conv(\mathcal{X})$ by definition of $Conv(\mathcal{X})$. This leads to the fact that precisely, all the new SMOTE samples are contained in $Conv(\mathcal{X})$. This implies $Supp(P_Z) \subseteq Conv(\mathcal{X})$.

□

B.2 Proof of Theorem 3.2

Proof of Theorem 3.2. We consider a single SMOTE iteration. Recall that the central point X_c (see Algorithm 1) is fixed, and thus denoted by x_c.

The random variables $X_{(1)}(x_c), \ldots, X_{(n-1)}(x_c)$ denote a reordering of the initial observations $X-1, X_2, \ldots, X_n$ such that

$$||X_{(1)}(x_c) - x_c|| \leq ||X_{(2)}(x_c) - x_c|| \leq \ldots \leq ||X_{(n-1)}(x_c) - x_c||.$$

For clarity, we remove the explicit dependence on x_c. Recall that SMOTE builds a linear interpolation between x_c and one of its K nearest neighbors chosen uniformly. Then the newly generated point Z satisfies

$$Z = (1-W)x_c + W\sum_{k=1}^{K} X_{(k)}\mathbb{1}_{\{I=k\}}, \tag{8}$$

where W is a uniform random variable over $[0,1]$, independent of $I, X_1, \ldots, X_n$, with I distributed as $\mathcal{U}(\{1, \ldots, K\})$.

From now, consider that the k-th nearest neighbor of x_c, $X_{(k)}(x_c)$, has been chosen (that is $I = k$). Then Z satisfies

$$\begin{aligned} Z &= (1-W)x_c + WX_{(k)} && (9)\\ &= x_c - Wx_c + WX_{(k)}, && (10)\end{aligned}$$

which implies

$$Z - x_c = W(X_{(k)} - x_c). \tag{11}$$

Let f_{Z-x_c}, f_W and $f_{X_{(k)}-x_c}$ be respectively the density functions of $Z-x_c$, W and $X_{(k)}-x_c$. Let $z, z_1, z_2 \in \mathbb{R}^d$. Recall that $z \leq z_1$ means that each component of z is lower than the corresponding component of z_1. Since W and $X_{(k)} - x_c$ are independent, we have,

$$\begin{aligned} \mathbb{P}(z_1 \leq Z - x_c \leq z_2) &= \int_{w\in\mathbb{R}}\int_{x\in\mathbb{R}^d} f_{W,X_{(k)}-x_c}(w,x)\mathbb{1}_{\{z_1\leq wx\leq z_2\}}\mathrm{d}w\mathrm{d}x && (12)\\ &= \int_{w\in\mathbb{R}}\int_{x\in\mathbb{R}^d} f_W(w)f_{X_{(k)}-x_c}(x)\mathbb{1}_{\{z_1\leq wx\leq z_2\}}\mathrm{d}w\mathrm{d}x && (13)\\ &= \int_{w\in\mathbb{R}} f_W(w)\left(\int_{x\in\mathbb{R}^d} f_{X_{(k)}-x_c}(x)\mathbb{1}_{\{z_1\leq wx\leq z_2\}}\mathrm{d}x\right)\mathrm{d}w. && (14)\end{aligned}$$

Besides, let $u = wx$. Then $x = (\frac{u_1}{w}, \ldots, \frac{u_d}{w})^T$.The Jacobian of such transformation equals:

$$\begin{vmatrix} \frac{\partial x_1}{\partial u_1} & \cdots & \frac{\partial x_1}{\partial u_d} \\ \vdots & \ddots & \vdots \\ \frac{\partial x_d}{\partial u_1} & \cdots & \frac{\partial x_d}{\partial u_d} \end{vmatrix} = \begin{vmatrix} \frac{1}{w} & & 0 \\ & \ddots & \\ 0 & \cdots & \frac{1}{w} \end{vmatrix} = \frac{1}{w^d} \tag{15}$$

Therefore, we have $x = u/w$ and $\mathrm{d}x = \mathrm{d}u/w^d$, which leads to

$$\mathbb{P}(z_1 \leq Z - x_c \leq z_2) \tag{16}$$

$$= \int_{w\in\mathbb{R}} \frac{1}{w^d} f_W(w) \left(\int_{u\in\mathbb{R}^d} f_{X_{(k)}-x_c}\left(\frac{u}{w}\right) \mathbb{1}_{\{z_1\leq u\leq z_2\}} \mathrm{d}u \right) \mathrm{d}w. \tag{17}$$

Note that a random variable Z' with density function

$$f_{Z'}(z') = \int_{w\in\mathbb{R}} \frac{1}{w^d} f_W(w) f_{X_{(k)}-x_c}\left(\frac{z'}{w}\right) \mathrm{d}w \tag{18}$$

satisfies, for all $z_1, z_2 \in \mathbb{R}^d$,

$$\mathbb{P}(z_1 \leq Z - x_c \leq z_2) = \int_{w\in\mathbb{R}} \frac{1}{w^d} f_W(w) \left(\int_{u\in\mathbb{R}^d} f_{X_{(k)}-x_c}\left(\frac{u}{w}\right) \mathbb{1}_{\{z_1\leq u\leq z_2\}} \mathrm{d}u \right) \mathrm{d}w. \tag{19}$$

Therefore, the variable $Z - x_c$ admits the following density

$$f_{Z-x_c}(z'|X_c = x_c, I = k) = \int_{w\in\mathbb{R}} \frac{1}{w^d} f_W(w) f_{X_{(k)}-x_c}\left(\frac{z'}{w}\right) \mathrm{d}w. \tag{20}$$

Since W follows a uniform distribution on $[0, 1]$, we have

$$f_{Z-x_c}(z'|X_c = x_c, I = k) = \int_0^1 \frac{1}{w^d} f_{X_{(k)}-x_c}\Big(\frac{z'}{w}\Big) \mathrm{d}w. \tag{21}$$

The density $f_{X_{(k)}-x_c}$ of the k-th nearest neighbor of x_c can be computed exactly [see, Lemma 6.1 in Berrett, 2017], that is

$$f_{X_{(k)}-x_c}(u) = (n-1)\binom{n-2}{k-1} f_X(x_c + u) \big[\mu_X\left(B(x_c, ||u||)\right)\big]^{k-1} \times \big[1 - \mu_X\left(B(x_c, ||u||)\right)\big]^{n-k-1}, \tag{22}$$

where

$$\mu_X\left(B(x_c, ||u||)\right) = \int_{B(x_c,\|u\|)} f_X(x) \mathrm{d}x. \tag{23}$$

We recall that $B(x_c, \|u\|)$ is the ball centered on x_c and of radius $\|u\|$. Hence we have

$$f_{X_{(k)}-x_c}(u) = (n-1)\binom{n-2}{k-1} f_X(x_c + u) \mu_X\left(B(x_c, ||u||)\right)^{k-1} \left[1 - \mu_X\left(B(x_c, ||u||)\right)\right]^{n-k-1}. \tag{24}$$

Since $Z - x_c$ is a translation of the random variable Z, we have

$$f_Z(z|X_c = x_c, I = k) = f_{Z-x_c}(z - x_c|X_c = x_c, I = k). \tag{25}$$

Injecting Equation (24) in Equation (21), we obtain

$$f_Z(z|X_c = x_c, I = k) \tag{26}$$

$$= f_{Z-x_c}(z - x_c|X_c = x_c, I = k) \tag{27}$$

$$= \int_0^1 \frac{1}{w^d} f_{X_{(k)}-x_c}\Big(\frac{z - x_c}{w}\Big) \mathrm{d}w \tag{28}$$

$$= (n-1)\binom{n-2}{k-1} \int_0^1 \frac{1}{w^d} f_X\left(x_c + \frac{z - x_c}{w}\right) \mu_X\left(B\left(x_c, \frac{||z - x_c||}{w}\right)\right)^{k-1} \tag{29}$$

$$\times \left[1 - \mu_X\left(B\left(x_c, \frac{||z - x_c||}{w}\right)\right)\right]^{n-k-1} \mathrm{d}w \tag{30}$$

Recall that in SMOTE, k is chosen at random in $\{1, \dots, K\}$ through the uniform random variable I. So far, we have considered I fixed. Taking the expectation with respect to I, we have

$$f_Z(z|X_c = x_c) \tag{31}$$

$$= \sum_{k=1}^{K} f_Z(z|X_c = x_c, I = k)\mathbb{P}[I = k] \tag{32}$$

$$= \frac{1}{K}\sum_{k=1}^{K}\int_0^1 \frac{1}{w^d} f_{X_{(k)}-x_c}\Big(\frac{z-x_c}{w}\Big)\mathrm{d}w \tag{33}$$

$$= \frac{1}{K}\sum_{k=1}^{K}(n-1)\binom{n-2}{k-1}\int_0^1 \frac{1}{w^d} f_X\left(x_c + \frac{z-x_c}{w}\right)\mu_X\left(B\left(x_c, \frac{||z-x_c||}{w}\right)\right)^{k-1} \tag{34}$$

$$\times [1-\mu_X\left(B\left(x_c, \frac{||z-x_c||}{w}\right)\right)]^{n-k-1}\mathrm{d}w \tag{35}$$

$$= \frac{(n-1)}{K}\int_0^1 \frac{1}{w^d} f_X\left(x_c + \frac{z-x_c}{w}\right)\sum_{k=1}^{K}\binom{n-2}{k-1}\mu_X\left(B\left(x_c, \frac{||z-x_c||}{w}\right)\right)^{k-1} \tag{36}$$

$$\times [1-\mu_X\left(B\left(x_c, \frac{||z-x_c||}{w}\right)\right)]^{n-k-1}\mathrm{d}w \tag{37}$$

$$= \frac{(n-1)}{K}\int_0^1 \frac{1}{w^d} f_X\left(x_c + \frac{z-x_c}{w}\right)\sum_{k=0}^{K-1}\binom{n-2}{k}\mu_X\left(B\left(x_c, \frac{||z-x_c||}{w}\right)\right)^{k} \tag{38}$$

$$\times \left[1-\mu_X\left(B\left(x_c, \frac{||z-x_c||}{w}\right)\right)\right]^{n-k-2}\mathrm{d}w. \tag{39}$$

Note that the sum can be expressed as the cumulative distribution function of a Binomial distribution parameterized by $n-2$ and $\mu_X(B(x_c, \|z-x_c\|/w))$, so that

$$\sum_{k=0}^{K-1}\binom{n-2}{k}\mu_X\left(B\left(x_c, \frac{||z-x_c||}{w}\right)\right)^{k}\left[1-\mu_X\left(B\left(x_c, \frac{||z-x_c||}{w}\right)\right)\right]^{n-k-2} \tag{40}$$

$$=(n-K-1)\binom{n-2}{K-1}\mathcal{B}\left(n-K-1, K; 1-\mu_X\left(B\left(x_c, \frac{||z-x_c||}{w}\right)\right)\right), \tag{41}$$

(see Technical Lemma C.1 for details). We inject Equation (41) in Equation (31)

$$f_Z(z|X_c = x_c) = (n-K-1)\binom{n-1}{K}\int_0^1 \frac{1}{w^d} f_X\left(x_c + \frac{z-x_c}{w}\right)$$
$$\times \mathcal{B}\left(n-K-1, K; 1-\mu_X\left(B\left(x_c, \frac{||z-x_c||}{w}\right)\right)\right)\mathrm{d}w. \tag{42}$$

We know that

$$f_Z(z) = \int_{x_c\in\mathcal{X}} f_Z(z|X_c = x_c)f_X(x_c)\mathrm{d}x_c.$$

Combining this remark with the result of Equation (42) we get

$$f_Z(z) = (n-K-1)\binom{n-1}{K}\int_{x_c\in\mathcal{X}}\int_0^1 \frac{1}{w^d} f_X\left(x_c + \frac{z-x_c}{w}\right)$$
$$\times \mathcal{B}\left(n-K-1, K; 1-\mu_X\left(B\left(x_c, \frac{||z-x_c||}{w}\right)\right)\right) f_X(x_c)\mathrm{d}w\mathrm{d}x_c. \tag{43}$$

Link with Elreedy's formula According to the Elreedy formula

$$f_Z(z|X_c = x_c) = (n-K-1)\binom{n-1}{K}\int_{r=\|z-x_c\|}^{\infty} f_X\left(x_c + \frac{(z-x_c)r}{\|z-x_c\|}\right)\frac{r^{d-2}}{\|z-x_c\|^{d-1}}$$
$$\times \mathcal{B}\left(n-K-1, K; 1-\mu_X\left(B\left(x_c, r\right)\right)\right)\mathrm{d}r. \tag{44}$$

Now, let $r = \|z - x_c\|/w$ so that $\mathrm{d}r = -\|z - x_c\|\mathrm{d}w/w^2$. Thus,

$$
\begin{aligned}
& f_Z(z|X_c = x_c) \\
&= (n-K-1)\binom{n-1}{K}\int_0^1 f_X\left(x_c + \frac{z-x_c}{w}\right)\frac{1}{w^{d-2}}\frac{1}{\|z-x_c\|} && (45)\\
&\quad \times \mathcal{B}\left(n-K-1, K; 1-\mu_X\left(B\left(x_c, \frac{z-x_c}{w}\right)\right)\right)\frac{\|z-x_c\|}{w^2}\mathrm{d}w && (46)\\
&= (n-K-1)\binom{n-1}{K}\int_0^1 \frac{1}{w^d} f_X\left(x_c + \frac{z-x_c}{w}\right) \\
&\quad \times \mathcal{B}\left(n-K-1, K; 1-\mu_X\left(B\left(x_c, \frac{z-x_c}{w}\right)\right)\right)\mathrm{d}w. && (47)
\end{aligned}
$$

□

B.3 Proof of Theorem 3.3

Proof of Theorem 3.3. For any event A, B, we have

$$1 - \mathbb{P}[A \cap B] = \mathbb{P}[A^c \cup B^c] \leq \mathbb{P}[A^c] + \mathbb{P}[B^c], \tag{48}$$

which leads to

$$
\begin{aligned}
\mathbb{P}[A \cap B] &\geq 1 - \mathbb{P}[A^c] - \mathbb{P}[B^c] && (49)\\
&= \mathbb{P}[A] - \mathbb{P}[B^c]. && (50)
\end{aligned}
$$

By construction,

$$\|X_c - Z\| \leq \|X_c - X_{(K)}(X_c)\|. \tag{51}$$

Let $x \in \mathcal{X}$ and $\eta > 0$. Let $\alpha, \varepsilon > 0$. We have,

$$
\begin{aligned}
&\mathbb{P}[X_c \in B(x, \alpha - \varepsilon)] - \mathbb{P}[\|X_c - X_{(K)}(X_c)\| > \varepsilon] && (52)\\
&\leq \mathbb{P}[X_c \in B(x, \alpha - \varepsilon), \|X_c - X_{(K)}(X_c)\| \leq \varepsilon] && (53)\\
&\leq \mathbb{P}[X_c \in B(x, \alpha - \varepsilon), \|X_c - Z\| \leq \varepsilon] && (54)\\
&\leq \mathbb{P}[Z \in B(x, \alpha)]. && (55)
\end{aligned}
$$

Similarly, we have

$$
\begin{aligned}
&\mathbb{P}[Z \in B(x, \alpha)] - \mathbb{P}[\|X_c - X_{(K)}(X_c)\| > \varepsilon] && (56)\\
&\leq \mathbb{P}[Z \in B(x, \alpha), \|X_c - X_{(K)}(X_c)\| \leq \varepsilon] && (57)\\
&\leq \mathbb{P}[Z \in B(x, \alpha), \|X_c - Z\| \leq \varepsilon] && (58)\\
&\leq \mathbb{P}[X_c \in B(x, \alpha + \varepsilon)]. && (59)
\end{aligned}
$$

Since X_c admits a density, for all $\varepsilon > 0$ small enough

$$\mathbb{P}[X_c \in B(x, \alpha + \varepsilon)] \leq \mathbb{P}[X_c \in B(x, \alpha)] + \eta, \tag{60}$$

and

$$\mathbb{P}[X_c \in B(x, \alpha)] - \eta \leq \mathbb{P}[X_c \in B(x, \alpha - \varepsilon)]. \tag{61}$$

Let ε such that (60) and (61) are verified. According to Lemma 2.3 in Biau and Devroye [2015], since $X_1, \ldots, X_n$ are i.i.d., if K/n tends to zero as $n \to \infty$, we have

$$\mathbb{P}[\|X_c - X_{(K)}(X_c)\| > \varepsilon] \to 0. \tag{62}$$

Thus, for all n large enough,

$$\mathbb{P}[X_c \in B(x, \alpha)] - 2\eta \leq \mathbb{P}[Z \in B(x, \alpha)] \tag{63}$$

and

$$\mathbb{P}[Z \in B(x, \alpha)] \leq 2\eta + \mathbb{P}[X_c \in B(x, \alpha)]. \tag{64}$$

Finally, for all $\eta > 0$, for all n large enough, we obtain

$$\mathbb{P}[X_c \in B(x, \alpha)] - 2\eta \leq \mathbb{P}[Z \in B(x, \alpha)] \leq 2\eta + \mathbb{P}[X_c \in B(x, \alpha)], \tag{65}$$

which proves that

$$\mathbb{P}[Z \in B(x, \alpha)] \to \mathbb{P}[X_c \in B(x, \alpha)]. \tag{66}$$

Therefore, by the Monotone convergence theorem, for all Borel sets $B \subset \mathbb{R}^d$,

$$\mathbb{P}[Z \in B] \to \mathbb{P}[X_c \in B]. \tag{67}$$

□

B.4 Proof of Theorem 3.5

Proof of Theorem 3.5. Let $x_c \in \mathcal{X}$ be a central point in a SMOTE iteration. From Theorem 3.2, we have,

$$
\begin{aligned}
&f_Z(z|X_c = x_c) \\
&= (n-K-1)\binom{n-1}{K}\int_0^1 \frac{1}{w^d} f_X\left(x_c + \frac{z-x_c}{w}\right) \\
&\quad \times \mathcal{B}\left(n-K-1, K; 1-\mu_X\left(B\left(x_c, \frac{||z-x_c||}{w}\right)\right)\right) \mathrm{d}w \qquad (68) \\
&= (n-K-1)\binom{n-1}{K}\int_0^1 \frac{1}{w^d} f_X\left(x_c + \frac{z-x_c}{w}\right) \mathbb{1}_{\{x_c+\frac{z-x_c}{w}\in\mathcal{X}\}} \\
&\quad \times \mathcal{B}\left(n-K-1, K; 1-\mu_X\left(B\left(x_c, \frac{||z-x_c||}{w}\right)\right)\right) \mathrm{d}w. \qquad (69)
\end{aligned}
$$

Let $R \in \mathbb{R}$ such that $\mathcal{X} \subset \mathcal{B}(0,R)$. For all $u = x_c + \frac{z-x_c}{w}$, we have

$$
w = \frac{||z-x_c||}{||u-x_c||}. \qquad (70)
$$

If $u \in \mathcal{X}$, then $u \in \mathcal{B}(0,R)$. Besides, since $x_c \in \mathcal{X} \subset B(0,R)$, we have $||u-x_c|| < 2R$ and

$$
w > \frac{||z-x_c||}{2R}. \qquad (71)
$$

Consequently,

$$
\mathbb{1}_{\left\{x_c+\frac{z-x_c}{w}\in\mathcal{X}\right\}} \leq \mathbb{1}_{\left\{w>\frac{||z-x_c||}{2R}\right\}}. \qquad (72)
$$

So finally

$$
\mathbb{1}_{\left\{x_c+\frac{z-x_c}{w}\in\mathcal{X}\right\}} = \mathbb{1}_{\left\{x_c+\frac{z-x_c}{w}\in\mathcal{X}\right\}}\mathbb{1}_{\left\{w>\frac{||z-x_c||}{2R}\right\}}. \qquad (73)
$$

Hence,

$$
\begin{aligned}
f_Z(z|X_c = x_c) &= (n-K-1)\binom{n-1}{K}\int_0^1 \frac{1}{w^d} f_X\left(x_c + \frac{z-x_c}{w}\right) \mathbb{1}_{\left\{x_c+\frac{z-x_c}{w}\in\mathcal{X}\right\}}\mathbb{1}_{\left\{w>\frac{||z-x_c||}{2R}\right\}} \\
&\quad \times \mathcal{B}\left(n-K-1, K; 1-\mu_X\left(B\left(x_c, \frac{||z-x_c||}{w}\right)\right)\right) \mathrm{d}w \qquad (74) \\
&= (n-K-1)\binom{n-1}{K}\int_{\frac{||z-x_c||}{2R}}^1 \frac{1}{w^d} f_X\left(x_c + \frac{z-x_c}{w}\right) \\
&\quad \times \mathcal{B}\left(n-K-1, K; 1-\mu_X\left(B\left(x_c, \frac{||z-x_c||}{w}\right)\right)\right) \mathrm{d}w. \qquad (75)
\end{aligned}
$$

Now, let $0 < \alpha \leq 2R$ and $z \in \mathbb{R}^d$ such that $||z-x_c|| > \alpha$. In such a case, $w > \frac{\alpha}{2R}$ and:

$$
\begin{aligned}
&f_Z(z|X_c = x_c) \qquad (76) \\
&= (n-K-1)\binom{n-1}{K}\int_{\frac{\alpha}{2R}}^1 \frac{1}{w^d} f_X\left(x_c + \frac{z-x_c}{w}\right) \\
&\quad \times \mathcal{B}\left(n-K-1, K; 1-\mu_X\left(B\left(x_c, \frac{||z-x_c||}{w}\right)\right)\right) \mathrm{d}w \qquad (77) \\
&\leq (n-K-1)\binom{n-1}{K}\int_{\frac{\alpha}{2R}}^1 \frac{1}{w^d} f_X\left(x_c + \frac{z-x_c}{w}\right) \mathcal{B}\left(n-K-1, K; 1-\mu_X\left(B\left(x_c, \alpha\right)\right)\right) \mathrm{d}w. \qquad (78)
\end{aligned}
$$

Let $\mu \in [0,1]$ and S_n be a binomial random variable of parameters $(n-1,\mu)$. For all K,

$$\mathbb{P}[S_n \leq K] = (n-K-1)\binom{n-1}{K}\mathcal{B}(n-K-1,K;1-\mu). \tag{79}$$

According to Hoeffding's inequality, we have, for all $K \leq (n-1)\mu$,

$$\mathbb{P}[S_n \leq K] \leq \exp\left(-2(n-1)\left(\mu - \frac{K}{n-1}\right)^2\right). \tag{80}$$

Thus, for all $z \notin B(x_c,\alpha)$, for all $K \leq (n-1)\mu_X(B(x_c,\alpha))$,

$$\begin{aligned}
&f_Z(z|X_c = x_c) && (81)\\
&\leq \exp\left(-2(n-1)\left(\mu_X(B(x_c,\alpha)) - \frac{K}{n-1}\right)^2\right)\int_{\frac{\alpha}{2R}}^1 \frac{1}{w^d} f_X\left(x_c + \frac{z-x_c}{w}\right)\mathrm{d}w && (82)\\
&\leq C_2 \exp\left(-2(n-1)\left(\mu_X(B(x_c,\alpha)) - \frac{K}{n-1}\right)^2\right)\int_{\frac{\alpha}{2R}}^1 \frac{1}{w^d}\mathrm{d}w && (83)\\
&\leq C_2\eta(\alpha,R)\exp\left(-2(n-1)\left(\mu_X(B(x_c,\alpha)) - \frac{K}{n-1}\right)^2\right), && (84)
\end{aligned}$$

with

$$\eta(\alpha,R) = \begin{cases} \ln\left(\frac{2R}{\alpha}\right) & \text{if } d=1 \\ \frac{1}{d-1}\left(\left(\frac{2R}{\alpha}\right)^{d-1}-1\right) & \text{otherwise} \end{cases}.$$

Letting

$$\epsilon(n,\alpha,K,x_c) = C_2\eta(\alpha,R)\exp\left(-2(n-1)\left(\mu_X(B(x_c,\alpha)) - \frac{K}{n-1}\right)^2\right), \tag{85}$$

we have, for all $\alpha \in (0,2R)$, for all $K \leq (n-1)\mu_X(B(x_c,\alpha))$,

$$\begin{aligned}
\mathbb{P}(|Z-X_c| \geq \alpha | X_c = x_c) &= \int_{z\notin\mathcal{B}(x_c,\alpha), z\in\mathcal{X}} f_Z(z|X_c=x_c)\mathrm{d}z && (86)\\
&\leq \int_{z\notin\mathcal{B}(x_c,\alpha), z\in\mathcal{X}} \varepsilon(n,\alpha,K,x_c)\mathrm{d}z && (87)\\
&= \varepsilon(n,\alpha,K,x_c)\int_{z\notin\mathcal{B}(x_c,\alpha), z\in\mathcal{X}} \mathrm{d}z && (88)\\
&\leq c_d R^d \varepsilon(n,\alpha,K,x_c), && (89)
\end{aligned}$$

as $\mathcal{X} \subset B(0,R)$. Since $x_c \in \mathcal{X}$, by definition of the support, we know that for all $\rho > 0$, $\mu_X(B(x_c,\rho)) > 0$. Thus, $\mu_X(B(x_c,\alpha)) > 0$. Consequently, $\varepsilon(n,\alpha,K,x_c)$ tends to zero, as K/n tends to zero. □

B.5 Proof of Theorem 3.6

We adapt the proof of Theorem 2.1 and Theorem 2.4 in Biau and Devroye [2015] to the case where X belongs to $B(0,R)$. We prove the following result.

Lemma B.1. *Let X takes values in $B(0,R)$. For all $d \geq 2$,*

$$\mathbb{E}[\|X_{(1)}(X) - X\|_2^2] \leq 36R^2\left(\frac{k}{n+1}\right)^{2/d}, \tag{90}$$

where $X_{(1)}(X)$ is the nearest neighbor of X among $X_1,\ldots,X_n$.

Proof of Theorem B.1. Let us denote by $X_{(i,1)}$ the nearest neighbor of X_i among $X_1, \ldots, X_{i-1}, X_{i+1}, \ldots, X_{n+1}$. By symmetry, we have

$$\mathbb{E}[\|X_{(1)}(X) - X\|_2^2] = \frac{1}{n+1} \sum_{i=1}^{n+1} \mathbb{E}\|X_{(i,1)} - X_i\|_2^2. \tag{91}$$

Let $R_i = \|X_{(i,1)} - X_i\|_2$ and $B_i = \{x \in \mathbb{R}^d : \|x - X_i\| < R_i/2\}$. By construction, B_i are disjoint. Since $R_i \leq 2R$, we have

$$\cup_{i=1}^{n+1} B_i \subset B(0, 3R), \tag{92}$$

which implies,

$$\mu\left(\cup_{i=1}^{n+1} B_i\right) \leq (3R)^d c_d. \tag{93}$$

Thus, we have

$$\sum_{i=1}^{n+1} c_d \left(\frac{R_i}{2}\right)^d \leq (3R)^d c_d. \tag{94}$$

Besides, for all $d \geq 2$, we have

$$\left(\frac{1}{n+1} \sum_{i=1}^{n+1} R_i^2\right)^{d/2} \leq \frac{1}{n+1} \sum_{i=1}^{n+1} R_i^d, \tag{95}$$

which leads to

$$\begin{aligned}
\mathbb{E}[\|X_{(1)}(X) - X\|_2^2] &= \frac{1}{n+1} \sum_{i=1}^{n+1} \mathbb{E}\|X_{(i,1)} - X_i\|_2^2 && (96)\\
&= \mathbb{E}\left[\frac{1}{n+1} \sum_{i=1}^{n+1} R_i^2\right] && (97)\\
&\leq \left(\frac{(6R)^d}{n+1}\right)^{2/d} && (98)\\
&\leq 36R^2 \left(\frac{1}{n+1}\right)^{2/d}. && (99)
\end{aligned}$$

□

Lemma B.2. *Let X takes values in $B(0, R)$. For all $d \geq 2$,*

$$\mathbb{E}[\|X_{(k)}(X) - X\|_2^2] \leq (2^{1+2/d})36R^2 \left(\frac{k}{n}\right)^{2/d}, \tag{100}$$

where $X_{(k)}(X)$ is the nearest neighbor of X among $X_1, \ldots, X_n$.

Proof of Theorem B.2. Set $d \geq 2$. Recall that $\mathbb{E}[\|X_{(k)}(X) - X\|_2^2] \leq 4R^2$. Besides, for all $k > n/2$, we have

$$\begin{aligned}
(2^{1+2/d})36R^2 \left(\frac{k}{n}\right)^{2/d} &> (2^{1+2/d})36R^2 \left(\frac{1}{2}\right)^{2/d} && (101)\\
&> 72R^2 && (102)\\
&> \mathbb{E}[\|X_{(k)}(X) - X\|_2^2]. && (103)
\end{aligned}$$

Thus, the result is trivial for $k > n/2$. Set $k \leq n/2$. Now, following the argument of Theorem 2.4 in Biau and Devroye [2015], let us partition the set $\{X_1, \ldots, X_n\}$ into $2k$ sets of sizes $n_1, \ldots, n_{2k}$ with

$$\sum_{j=1}^{2k} n_j = n \quad \text{and} \quad \left\lfloor \frac{n}{2k} \right\rfloor \leq n_j \leq \left\lfloor \frac{n}{2k} \right\rfloor + 1. \tag{104}$$

Let $X^{\star}_{(1)}(j)$ be the nearest neighbor of X among all X_i in the jth group. Note that

$$\|X_{(k)}(X) - X\|^2 \leq \frac{1}{k}\sum_{j=1}^{2k} \|X^{\star}_{(1)}(j) - X\|^2, \tag{105}$$

since at least k of these nearest neighbors have values larger than $\|X_{(k)}(X) - X\|^2$. By Theorem B.1, we have

$$\|X_{(k)}(X) - X\|^2 \leq \frac{1}{k}\sum_{j=1}^{2k} 36R^2 \left(\frac{1}{n_j + 1}\right)^{2/d} \tag{106}$$

$$\leq \frac{1}{k}\sum_{j=1}^{2k} 36R^2 \left(\frac{2k}{n}\right)^{2/d} \tag{107}$$

$$\leq 2^{1+2/d} \times 36R^2 \left(\frac{k}{n}\right)^{2/d}. \tag{108}$$

□

Proof of Theorem 3.6. Let $d \geq 2$. By Markov's inequality, for all $\varepsilon > 0$, we have

$$\mathbb{P}\left[\|X_{(k)}(X) - X\|_2 > \varepsilon\right] \leq \frac{\mathbb{E}[\|X_{(k)}(X) - X\|_2^2]}{\varepsilon^2}. \tag{109}$$

Let $\gamma \in (0, 1/d)$ and $\varepsilon = 12R(k/n)^{\gamma}$, we have

$$\mathbb{P}\left[\|X_{(k)}(X) - X\|_2 > 12R(k/n)^{\gamma}\right] \leq \left(\frac{k}{n}\right)^{2/d - 2\gamma}. \tag{110}$$

Noticing that, by construction of a SMOTE observation $Z_{K,n}$, we have

$$\|Z_{K,n} - X\|_2^2 \leq \|X_{(K)}(X) - X\|_2^2. \tag{111}$$

Thus,

$$\mathbb{P}\left[\|Z_{K,n} - X\|_2^2 > 12R(k/n)^{\gamma}\right] \leq \mathbb{P}\left[\|X_{(K)}(X) - X\|_2^2 > 12R(k/n)^{1/d}\right] \tag{112}$$

$$\leq \left(\frac{k}{n}\right)^{2/d - 2\gamma}. \tag{113}$$

□

B.6 Proof of Theorem 3.7

Proof of Theorem 3.7. Let $\varepsilon > 0$ and $z \in B(0, R)$ such that $\|z\| \geq R - \varepsilon$. Let $A_{\varepsilon} = \{x \in B(0, R), \langle x - z, z\rangle \leq 0\}$. Let $0 < \alpha < 2R$ and $\tilde{A}_{\alpha,\varepsilon} = A_{\varepsilon} \cap \{x, \|z - x\| \geq \alpha\}$. An illustration is displayed in Figure 4.

We have

$$f_Z(z) = \int_{x_c \in \tilde{A}_{\alpha,\varepsilon}} f_Z(z|X_c = x_c) f_X(x_c) \mathrm{d}x_c + \int_{x_c \in \tilde{A}^c_{\alpha,\varepsilon}} f_Z(z|X_c = x_c) f_X(x_c) \mathrm{d}x_c \tag{114}$$

First term Let $x_c \in \tilde{A}_{\alpha,\varepsilon}$. In order to have $x_c + \frac{z - x_c}{w} = z + \left(-1 + \frac{1}{w}\right)(z - x_c) \in B(0, R)$, it is necessary that

$$\left(-1 + \frac{1}{w}\right)\|z - x_c\| \leq \sqrt{2\varepsilon R} \tag{115}$$

which leads to

$$w \geq \frac{1}{1 + \frac{\sqrt{2\varepsilon R}}{\|z - x_c\|}} \tag{116}$$

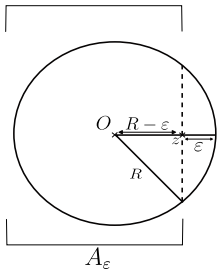

Figure 4: Illustration of Theorem 3.7.

Since $x_c \in \tilde{A}_{\alpha,\varepsilon}$, we have $\|x_c - z\| \geq \alpha$. Thus, according to inequality (116), $x_c + \frac{z-x_c}{w} \in B(0,R)$ implies

$$w \geq \frac{1}{1+\frac{\sqrt{2\varepsilon R}}{\alpha}}. \tag{117}$$

Recall that $x_c + \frac{z-x_c}{w} \in \mathcal{X}$. Consequently, according to Theorem 3.2, for all $x_c \in \tilde{A}_{\alpha,\varepsilon}$,

$$\begin{aligned}
&f_Z(z|X_c = x_c) && (118)\\
&= (n-K-1)\binom{n-1}{K}\int_0^1 \frac{1}{w^d} f_X\left(x_c + \frac{z-x_c}{w}\right)\\
&\qquad \times \mathcal{B}\left(n-K-1, K; 1-\mu_X\left(B\left(x_c, \frac{||z-x_c||}{w}\right)\right)\right)\mathrm{d}w && (119)\\
&\leq C_2(n-K-1)\binom{n-1}{K}\int_{\frac{1}{1+\frac{\sqrt{2\varepsilon R}}{\alpha}}}^1 \frac{1}{w^d}\mathcal{B}\left(n-K-1, K; 1-\mu_X\left(B\left(x_c, \frac{||z-x_c||}{w}\right)\right)\right)\mathrm{d}w. && (120)
\end{aligned}$$

Besides,

$$\begin{aligned}
&(n-K-1)\binom{n-1}{K}\mathcal{B}\left(n-K-1, K; 1-\mu_X\left(B\left(x_c, \frac{||z-x_c||}{w}\right)\right)\right) && (121)\\
&= \left(\frac{n-1}{K}\right)(n-K-1)\binom{n-2}{K-1}\mathcal{B}\left(n-K-1, K; 1-\mu_X\left(B\left(x_c, \frac{||z-x_c||}{w}\right)\right)\right) && (122)\\
&\leq \frac{n-1}{K}, && (123)
\end{aligned}$$

according to Lemma C.1. Thus,

$$\begin{aligned}
f_Z(z|X_c = x_c) &\leq C_2\left(\frac{n-1}{K}\right)\int_{\frac{1}{1+\frac{\sqrt{2\varepsilon R}}{\alpha}}}^1 \frac{1}{w^d}\mathrm{d}w && (124)\\
&\leq C_2\left(\frac{n-1}{K}\right)\eta(\alpha, R), && (125)
\end{aligned}$$

with

$$\eta(\alpha,R) = \begin{cases} \ln\left(1+\frac{\sqrt{2\varepsilon R}}{\alpha}\right) & \text{if } d=1\\ \frac{1}{d-1}\left(\left(1+\frac{\sqrt{2\varepsilon R}}{\alpha}\right)^{d-1}-1\right) & \text{otherwise} \end{cases}.$$

Second term According to Theorem 3.2, we have

$$f_Z(z|X_c = x_c) = (n-K-1)\binom{n-1}{K}\int_0^1 \frac{1}{w^d} f_X\left(x_c + \frac{z-x_c}{w}\right) \times \mathcal{B}\left(n-K-1, K; 1-\mu_X\left(B\left(x_c, \frac{||z-x_c||}{w}\right)\right)\right) \mathrm{d}w \tag{126}$$

$$\leq \left(\frac{n-1}{K}\right)\int_0^1 \frac{1}{w^d} f_X\left(x_c + \frac{z-x_c}{w}\right) \mathrm{d}w \tag{127}$$

Since $\mathcal{X} \subset B(0,R)$, all points $x, z \in \mathcal{X}$ satisfy $\|x-z\| \leq 2R$. Consequently, if $\|z-x_c\|/w > 2R$,

$$x_c + \frac{\|z-x_c\|}{w} \notin \mathcal{X}. \tag{128}$$

Hence, for all $w \leq \|z-x_c\|/2R$,

$$f_X\left(x_c + \frac{z-x_c}{w}\right) = 0. \tag{129}$$

Plugging this equality into (127), we have

$$f_Z(z|X_c = x_c) \tag{130}$$

$$\leq \left(\frac{n-1}{K}\right)\int_{\|z-x_c\|/2R}^1 \frac{1}{w^d} f_X\left(x_c + \frac{z-x_c}{w}\right) \mathrm{d}w \tag{131}$$

$$\leq C_2\left(\frac{n-1}{K}\right)\int_{\|z-x_c\|/2R}^1 \frac{1}{w^d}\mathrm{d}w \tag{132}$$

$$\leq C_2\left(\frac{n-1}{K}\right)\left[-\frac{1}{d-1}w^{-d+1}\right]_{\|z-x_c\|/2R}^1 \tag{133}$$

$$\leq C_2\left(\frac{n-1}{K}\right)\frac{(2R)^{d-1}}{d-1}\frac{1}{\|z-x_c\|^{d-1}}. \tag{134}$$

Besides, note that, for all $\alpha > 0$, we have

$$\int_{B(z,\alpha)} \frac{1}{\|z-x_c\|^{d-1}} f_X(x_c)\mathrm{d}x_c \tag{135}$$

$$\leq C_2 \int_{B(0,\alpha)} \frac{1}{r^{d-1}} r^{d-1}\sin^{d-2}(\varphi_1)\sin^{d-3}(\varphi_2)\ldots\sin(\varphi_{d-2})\mathrm{d}r\mathrm{d}\varphi_1\ldots\mathrm{d}\varphi_{d-2}, \tag{136}$$

where $r, \varphi_1, \ldots, \varphi_{d-2}$ are the spherical coordinates. A direct calculation leads to

$$\int_{B(z,\alpha)} \frac{1}{\|z-x_c\|^{d-1}} f_X(x_c)\mathrm{d}x_c$$

$$\leq C_2 \int_0^\alpha \mathrm{d}r \int_{S(0,\alpha)} \sin^{d-2}(\varphi_1)\sin^{d-3}(\varphi_2)\ldots\sin(\varphi_{d-2})\mathrm{d}\varphi_1\ldots\mathrm{d}\varphi_{d-2} \tag{137}$$

$$\leq \frac{2C_2\pi^{d/2}}{\Gamma(d/2)}\alpha, \tag{138}$$

as

$$\int_{S(0,\alpha)} \sin^{d-2}(\varphi_1)\sin^{d-3}(\varphi_2)\ldots\sin(\varphi_{d-2})\mathrm{d}\varphi_1\ldots\mathrm{d}\varphi_{d-2} \tag{139}$$

is the surface of the S^{d-1} sphere. Finally, for all $z \in \mathcal{X}$, for all $\alpha > 0$, and for all K, N such that $1 \leq K \leq N$, we have

$$\int_{B(z,\alpha)} f_Z(z|X_c = x_c) f_X(x_c)\mathrm{d}x_c \leq \frac{2C_2^2(2R)^{d-1}\pi^{d/2}}{(d-1)\Gamma(d/2)}\left(\frac{n-1}{K}\right)\alpha. \tag{140}$$

Final result Using Figure 4 and Pythagore's Theorem, we have $a^2 \leq \sqrt{2\varepsilon R}$. Let $d > 1$ and $\epsilon > 0$. Then we have for all α such that $\alpha > a$.

$$f_Z(z) \tag{141}$$

$$= \int_{x_c \in \tilde{A}_{\alpha,\varepsilon}} f_Z(z|X_c = x_c) f_X(x_c) \mathrm{d}x_c + \int_{x_c \in \tilde{A}^c_{\alpha,\varepsilon}} f_Z(z|X_c = x_c) f_X(x_c) \mathrm{d}x_c \tag{142}$$

$$\leq \frac{C_2}{d-1} \left(\left(1 + \frac{\sqrt{2\varepsilon R}}{\alpha} \right)^{d-1} - 1 \right) \left(\frac{n-1}{K} \right) + \frac{2C_2^2 (2R)^{d-1} \pi^{d/2}}{(d-1)\Gamma(d/2)} \left(\frac{n-1}{K} \right) \alpha \tag{143}$$

$$= \frac{C_2}{d-1} \left(\frac{n-1}{K} \right) \left[\left(\left(1 + \frac{\sqrt{2\varepsilon R}}{\alpha} \right)^{d-1} - 1 \right) + \frac{2C_2 (2R)^{d-1} \pi^{d/2}}{\Gamma(d/2)} \alpha \right], \tag{144}$$

But this inequality is true if $\alpha \geq a$. We know that $(1+x)^{d-1} \leq (2^{d-1} - 1)x + 1$ for $x \in [0, 1]$ and $d - 1 \geq 0$. Then, for α such that $\frac{\sqrt{2\varepsilon R}}{\alpha} \leq 1$,

$$f_Z(z) \tag{145}$$

$$\leq \frac{C_2}{d-1} \left(\frac{n-1}{K} \right) \left[\left(\left((2^{d-1} - 1) \frac{\sqrt{2\varepsilon R}}{\alpha} + 1 \right) - 1 \right) + \frac{2C_2 (2R)^{d-1} \pi^{d/2}}{\Gamma(d/2)} \alpha \right] \tag{146}$$

$$\leq \frac{C_2}{d-1} \left(\frac{n-1}{K} \right) \left[\left((2^{d-1} - 1) \frac{\sqrt{2\varepsilon R}}{\alpha} \right) + \frac{2C_2 (2R)^{d-1} \pi^{d/2}}{\Gamma(d/2)} \alpha \right]. \tag{147}$$

Since $\frac{\sqrt{2\varepsilon R}}{\alpha} \leq 1$, then $\alpha \geq \sqrt{2\varepsilon R} \geq a$. So our initial condition on α to get the upper bound of the second term is still true. Now, we choose α such that,

$$(2^{d-1} - 1) \frac{\sqrt{2\varepsilon R}}{\alpha} \leq \frac{2C_2 (2R)^{d-1} \pi^{d/2}}{\Gamma(d/2)} \alpha, \tag{148}$$

which leads to the following condition

$$\alpha \geq \left(\frac{\Gamma(d/2)(2^{d-1} - 1)\sqrt{2\varepsilon R}}{2C_2 (2R)^{d-1} \pi^{d/2}} \right)^{1/2}, \tag{149}$$

assuming that

$$\left(\frac{\varepsilon}{R} \right)^{1/2} \leq \frac{1}{\sqrt{2} d C_2} Vol(B_d(0, 1)). \tag{150}$$

Finally, for

$$\alpha = \left(\frac{\Gamma(d/2)(2^{d-1} - 1)\sqrt{2\varepsilon R}}{2C_2 (2R)^{d-1} \pi^{d/2}} \right)^{1/2}, \tag{151}$$

we have,

$$f_Z(z) \leq \frac{C_2}{d-1} \left(\frac{n-1}{K} \right) \left[\frac{4C_2 (2R)^{d-1} \pi^{d/2}}{\Gamma(d/2)} \alpha \right] \tag{152}$$

$$\leq \frac{C_2}{d-1} \left(\frac{n-1}{K} \right) \left[\frac{4C_2 (2R)^{d-1} \pi^{d/2}}{\Gamma(d/2)} \left(\frac{\Gamma(d/2)(2^{d-1} - 1)\sqrt{2\varepsilon R}}{2C_2 (2R)^{d-1} \pi^{d/2}} \right)^{1/2} \right] \tag{153}$$

$$= 2^{d+2} \left(\frac{n-1}{K} \right) \left(\frac{C_2^3 Vol(B_d(0, 1))}{d} \right)^{1/2} \left(\frac{\varepsilon}{R} \right)^{1/4}. \tag{154}$$

□

C Technical lemmas

C.0.1 Cumulative distribution function of a binomial law

Lemma C.1 (Cumulative distribution function of a binomial distribution)**.** *Let X be a random variable following a binomial law of parameter $n \in \mathbf{N}$ and $p \in [0,1]$. The cumulative distribution function F of X can be expressed as Wadsworth et al. [1961]:*

(i)

$$F(k;n,p) = \mathbb{P}(X \leq k) = \sum_{i=0}^{\lfloor k \rfloor} \binom{n}{i} p^i (1-p)^{n-i},$$

(ii)

$$\begin{aligned} F(k;n,p) &= (n-k)\binom{n}{k} \int_0^{1-p} t^{n-k-1}(1-t)^k \mathrm{d}t \\ &= (n-k)\binom{n}{k} \mathcal{B}(n-k, k+1; 1-p), \end{aligned}$$

with $\mathcal{B}(a,b;x) = \int_{t=0}^{x} t^{a-1}(1-t)^{b-1}\mathrm{d}t$, the incomplete beta function.

Proof. see Wadsworth et al. [1961]. □

C.0.2 Upper bounds for the incomplete beta function

Lemma C.2. *Let $B(a,b;x) = \int_{t=0}^{x} t^{a-1}(1-t)^{b-1}\mathrm{d}t$, be the incomplete beta function. Then we have*

$$\frac{x^a}{a} \leq B(a,b;x) \leq x^{a-1}\left(\frac{1-(1-x)^b}{b}\right),$$

for $a > 0$.

Proof. We have

$$\begin{aligned} B(a,b;x) &= \int_{t=0}^{x} t^{a-1}(1-t)^{b-1}\mathrm{d}t \\ &\leq \int_{t=0}^{x} x^{a-1}(1-t)^{b-1}\mathrm{d}t \\ &= x^{a-1}\int_{t=0}^{x} (1-t)^{b-1}\mathrm{d}t \\ &= x^{a-1}\left[(-1)\frac{(1-t)^b}{b}\right]_0^x \\ &= x^{a-1}\left[-\frac{(1-x)^b}{b} + \frac{1}{b}\right] \\ &= x^{a-1}\frac{1-(1-x)^b}{b}. \end{aligned}$$

On the other hand,

$$\begin{aligned} B(a,b;x) &= \int_{t=0}^{x} t^{a-1}(1-t)^{b-1}\mathrm{d}t \\ &\geq \int_{t=0}^{t} x^{a-1}\mathrm{d}t \\ &= \left[\frac{t^a}{a}\right]_0^x \\ &= \frac{x^a}{a} - \frac{0^a}{a} \\ &= \frac{x^a}{a}. \end{aligned}$$

□

C.0.3 Upper bounds for binomial coefficient

Lemma C.3. *For $k, n \in \mathbb{N}$ such that $k < n$, we have*

$$\binom{n}{k} \leq \left(\frac{en}{k}\right)^k. \tag{155}$$

Proof. We have,

$$\binom{n}{k} = \frac{n(n-1)\dots(n-k+1)}{k!} \leq \frac{n^k}{k!}. \tag{156}$$

Besides,

$$e^k = \sum_{i=0}^{+\infty} \frac{k^i}{i!} \Longrightarrow e^k \geq \frac{k^k}{k!} \Longrightarrow \frac{e^k}{k^k} \geq \frac{1}{k!}. \tag{157}$$

Hence,

$$\binom{n}{k} = \frac{n(n-1)\dots(n-k+1)}{k!} \leq \frac{n^k}{k!} \leq \left(\frac{en}{k}\right)^k. \tag{158}$$

□

C.0.4 Inequality $x \ln\left(\frac{1}{x}\right) \leq \sqrt{x}$

Lemma C.4. *For $x \in]0, +\infty[$,*

$$x \ln\left(\frac{1}{x}\right) \leq \sqrt{x}. \tag{159}$$

Proof. Let,

$$f(x) = \sqrt{x} - x \ln\left(\frac{1}{x}\right) \tag{160}$$

$$= \sqrt{x} + x \ln(x). \tag{161}$$

Then,

$$f^{'}(x) = \frac{1}{2\sqrt{x}} + \ln x + 1. \tag{162}$$

And,

$$f^{''}(x) = \frac{1}{x} - \frac{1}{4x^{3/2}}. \tag{163}$$

We have,

$$\begin{aligned} f^{''}(x) \geq 0 &\Longrightarrow \frac{1}{x} - \frac{1}{4x^{3/2}} \geq 0 \\ &\Longrightarrow \frac{1}{x} \geq \frac{1}{4x^{3/2}} \end{aligned} \tag{164}$$

Since $x \in]0, +\infty[$,

$$Equation\ (164) \Longrightarrow \frac{x^{3/2}}{x} \geq \frac{1}{4} \tag{165}$$

$$\Longrightarrow \sqrt{x} \geq \frac{1}{4} \tag{166}$$

$$\Longrightarrow x \geq \frac{1}{16}. \tag{167}$$

This result leads to,

x	0		$\frac{1}{16}$		$+\infty$
f''		$-$	0	$+$	
f'	$\searrow$		$2 + \ln(\frac{1}{16}) + 1$		$\nearrow$

(168)

We have $2 + \ln(\frac{1}{16}) + 1 > 0$. So $f^{'}(x) > 0$ for all $x \in]0, \infty[$. Furthermore $\lim_{x \to 0^+} f(x) = 0$, hence $f(x) > 0$ for all $x \in]0, \infty[$, therefore $\sqrt{x} > x \ln\left(\frac{1}{x}\right)$ for all $x \in]0, \infty[$.

□